

1 **Development and testing of scenarios for implementing land use and land cover changes during**
2 **the Holocene in Earth System Model Experiments**

3
4 Sandy P. Harrison¹, Marie-José Gaillard², Benjamin D. Stocker^{3,4}, Marc Vander Linden⁵, Kees Klein
5 Goldewijk^{6,7}, Oliver Boles⁸, Pascale Braconnot⁹, Andria Dawson¹⁰, Etienne Fluet-Chouinard¹¹, Jed
6 O. Kaplan^{12,13}, Thomas Kastner¹⁴, Francesco S.R. Pausata¹⁵, Erick Robinson¹⁶, Nicki J.
7 Whitehouse¹⁷, Marco Madella^{18,19,20}, Kathleen D. Morrison⁸

8
9 Ms for Geoscientific Model Development (PMIP special issue)

10
11 1: Department of Geography and Environmental Science, University of Reading, Reading, UK

12 2: Department of Biology and Environmental Science, Linnaeus University, Kalmar, Sweden

13 3: Ecological and Forestry Applications Research Centre, Cerdanyola del Vallès, Spain

14 4: Department of Earth System Science, Stanford University, Stanford, CA 94305, USA

15 5: Department of Archaeology, University of Cambridge, UK

16 6: PBL Netherlands Environmental Assessment Agency, The Hague, The Netherlands

17 7: Copernicus Institute of Sustainable Development, Utrecht University, The Netherlands

18 8: University Museum of Archaeology & Anthropology, University of Pennsylvania, Philadelphia,
19 USA

20 9: Laboratoire des Sciences du Climat et de l'Environnement, Gif-sur-Yvette, France

21 10: Department of General Education, Mount Royal University, Calgary, Canada

22 11: Department of Earth System Science, Stanford University, California, USA

23 12: Department of Earth Sciences, University of Hong Kong, Hong Kong

24 13: Institute of Geography, University of Augsburg, Augsburg, Germany

25 14: Senckenberg Biodiversity and Climate Research Centre, Frankfurt am Main, Germany

26 15: Centre ESCER, Department of Earth and Atmospheric Sciences, University of Quebec in
27 Montreal, Montreal, Canada

28 16: Department of Anthropology, University of Wyoming, Laramie, Wyoming, USA

29 17: School of Geography, Earth and Environmental Science, University of Plymouth, Plymouth,
30 UK

31 18: Department of Humanities (CaSEs), University Pompeu Fabra, Barcelona, Spain

32 19: ICREA Passeig Lluís Companys 23 08010 Barcelona, Spain

33 20: School of Geography, Archaeology and Environmental Studies, University of Witwatersrand,
34 Johannesburg, South Africa

35 **Abstract:** Anthropogenic changes in land use and land cover (LULC) during the pre-industrial
36 Holocene could have affected regional and global climate. Existing scenarios of LULC changes
37 during the Holocene are based on relatively simple assumptions and highly uncertain estimates of
38 population changes through time. Archaeological and palaeoenvironmental reconstructions have the
39 potential to refine these assumptions and estimates. The Past Global Changes (PAGES) LandCover6k
40 initiative is working towards improved reconstructions of LULC globally. In this paper, we document
41 the types of archaeological data that are being collated and how they will be used to improve LULC
42 reconstructions. Given the large methodological uncertainties involved, both in reconstructing LULC
43 from the archaeological data and in implementing these reconstructions into global scenarios of
44 LULC, we propose a protocol to evaluate the revised scenarios using independent pollen-based
45 reconstructions of land cover and climate. Further evaluation of the revised scenarios involves
46 carbon-cycle model simulations to determine whether the LULC reconstructions are consistent with
47 constraints provided by ice-core records of CO₂ evolution and modern-day LULC. Finally, the
48 protocol outlines how the improved LULC reconstructions will be used in palaeoclimate simulations
49 in the Palaeoclimate Modelling Intercomparison Project to quantify the magnitude of anthropogenic
50 impacts on climate through time and ultimately to improve the realism of Holocene climate
51 simulations.

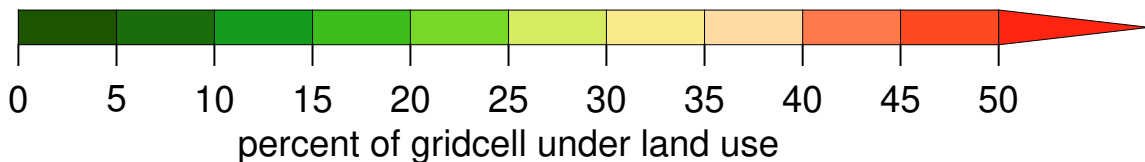
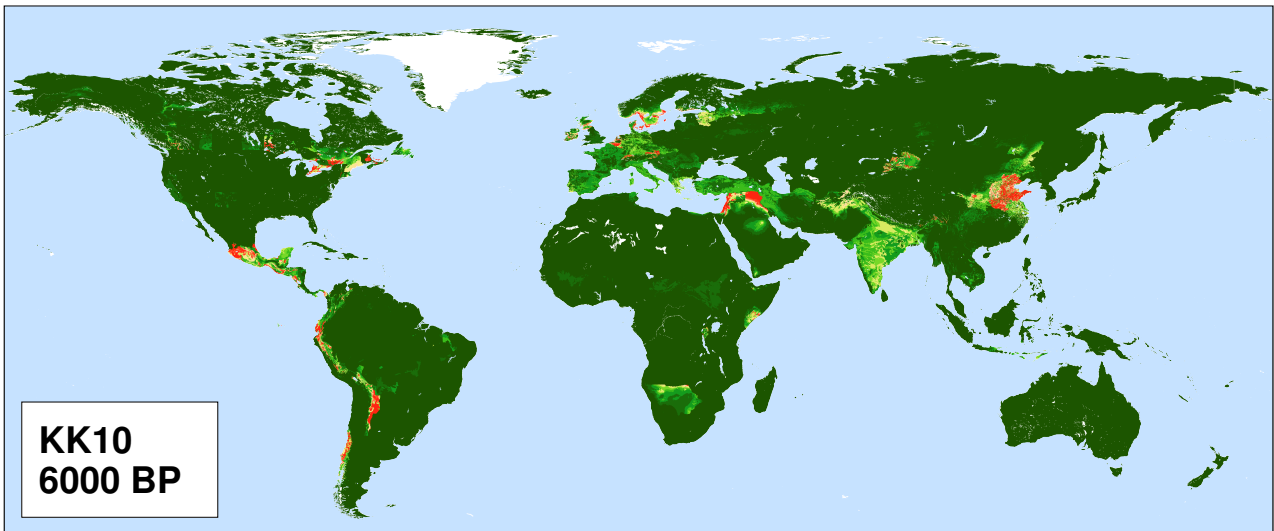
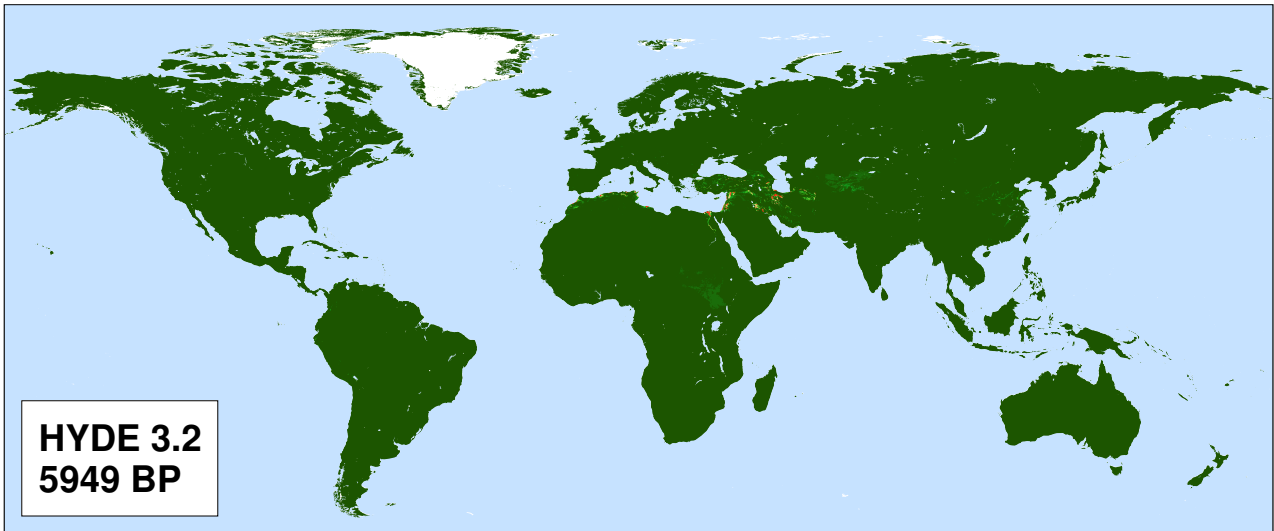
52

1 Introduction and Motivation

Today, ca 10% the ice-free land surface is estimated to be intensively managed and much of the remainder is under less intense anthropogenic use or influenced by human activities (Arneeth et al., 2019). Substantial transformations of natural ecosystems by humans began with the geographically diachronous shift from hunting and gathering characteristic of the Mesolithic to cultivation and more permanent settlement during the Neolithic period (Mazoyer and Roudart, 2006; Zohary et al., 2012; Tauger, 2013; Maezumi et al. 2018), although there is controversy about the relative importance of climate changes and human impact on landscape development both during and since that time. Resolving the uncertainty about the extent and timing of land use is important because changes in land cover as a result of land use (land use land cover: LULC) have the potential to impact climate and the carbon cycle. Direct climate impacts occur through changes in the surface-energy budget resulting from modifications of surface albedo, evapotranspiration, and canopy structure (biophysical impacts, e.g. Pongratz et al., 2010; Myhre et al., 2013; Perugini et al., 2017). LULC affects the carbon cycle through modifications in vegetation and soil carbon storage (biogeochemical impacts, e.g. Pongratz et al., 2010; Mahowald et al., 2017) and turnover times, which changes the C sink/source capacity of the terrestrial biosphere. LULC changes have contributed substantially to the increase in atmospheric greenhouse gases during the industrial period (Le Quéré et al., 2018). It has been suggested that greenhouse gas emissions associated with Neolithic LULC changes were sufficiently large to offset climate cooling after the Mid-Holocene (the overdue-glaciation hypothesis: Ruddiman 2003). Although this has been challenged for several reasons, including inconsistency with the land carbon balance derived from ice-core and peat records (e.g. Joos et al., 2004; Kaplan et al., 2011; Singarayer et al., 2011; Mitchell et al., 2013; Stocker et al. 2017), a LULC impact on climate in more recent millennia appears more plausible.

Climate model simulations have shown that LULC changes have discernible impacts on climate, both in regions with large prescribed changes in LULC and in teleconnected regions with no major local human activity (Vavrus et al., 2008; Pongratz et al., 2010; He et al., 2014; Smith et al., 2016). At the global scale, the biogeophysical effects of the accumulated LULC change during the Holocene which resulted in reconstructed land cover patterns in 1850 CE have been estimated to cause a slight cooling (0.17 °C) that is offset by the biogeochemical warming (0.9 °C), giving a net global warming (0.73 °C) (He et al., 2014). However, in these simulations, biophysical and biogeochemical effects were of comparable magnitude in the most intensively altered landscapes of Europe, Asia, and North America (He et al., 2014). Using parallel simulations, with and without LULC changes, Smith et al. (2016) showed that detectable temperature changes due to LULC could have occurred as early as 7000 years ago (7ka BP) in summer and throughout the year by 3ka BP. All of these conclusions, however, are obviously contingent on the imposed LULC forcing, which is highly uncertain.

There have been several attempts to map LULC changes through time (e.g. Ramankutty and Foley, 1999; Pongratz et al., 2008; Kaplan et al., 2011; Klein Goldewijk et al. 2011; Klein Goldewijk et al. 2017a, b). All of these reconstructions assume that anthropogenic land use is a function of population density and the suitability of land for crops and/or pasture. They then use estimates of regional population trends through time in combination with assumptions about per-capita land use and spatial land use allocation schemes to estimate anthropogenic changes in LULC across time and space. However, differences in the underlying assumptions about land-use per capita, which are generalized from limited and often site-specific data, have resulted in large differences in the final reconstructions (Gaillard et al., 2010; Kaplan et al., 2017). Hence, there are still very large uncertainties about the timing and magnitude of LULC changes, both at a global and at a regional scale (Figure 1).



103
104 **Figure 1:** Land use at ca 6000 years ago (6ka BP, 4000 years BCE) from the two widely used global
105 historical land-use scenarios HYDE 3.2 (top panel, Klein Goldewijk et al. 2017a) and KK10 (bottom
106 panel, Kaplan et al. 2011), illustrating the large disagreement between LULC scenarios at a regional
107 scale. In both scenarios, the land-sea mask and lake areas are for the present day.

108
109 There is a wealth of archaeological, historical and palaeo-vegetation data that could be used to
110 improve the relatively simple rules used to generate global LULC reconstructions. For example,
111 settlement density and numbers of radiocarbon-dated artifacts can be used to infer population sizes
112 and their temporal dynamics (Rick, 1987; Williams, 2012; Silva and Vander Linden, 2017).
113 Carbonised and waterlogged plant remains and animal bones can be used to infer the occurrence and
114 nature of agriculture at a site, although their presence provides no quantitative information about the
115 area under cultivation (Wright, 2003; Lyman 2008; Orton et al., 2016). Although the record of LULC
116 is likely to be patchy and incomplete, because of preservation and sampling issues, systematic use of
117 archaeological data is one important way to improve current LULC scenarios.
118

119 The Past Global Change (PAGES, <http://www.pastglobalchanges.org/>) LandCover6k Working
120 Group (<http://pastglobalchanges.org/ini/wg/landcover6k>) is currently working to develop a rigorous
121 and robust approach to provide data and data products that can be used to inform the development of
122 LULC scenarios (Gaillard et al., 2018). LULC changes are taken into account in climate-model
123 simulations currently being made in the current phase of the Coupled Model Intercomparison Project
124 (CMIP6) for the historic period and the future scenario runs (Eyring et al., 2016). They are also
125 included in climate-model simulations of the past millennium (Jungclaus et al., 2017), in order to
126 ensure that these runs mesh seamlessly with the historic simulations. However, the Land Use
127 Harmonisation data set (LUH2: Hurtt et al., 2017) only extends back to 850 CE and thus scenarios of
128 LULC changes are currently not included in the CMIP6 palaeoclimate simulations, including mid-
129 Holocene simulations, that are used as a test of how well state-of-the-art climate models reproduce
130 large climate changes. In this paper, we discuss how archaeological data will be used to improve
131 global LULC scenarios for the Holocene. Given that there are large uncertainties associated with the
132 primary data and further uncertainties may be introduced when this information is used to modify
133 existing LULC scenarios, we outline a series of tests that will be used to evaluate whether the revised
134 LULC scenarios are consistent with the changes implied by independent pollen-based reconstructions
135 of land cover and whether they produce more realistic estimates of both carbon cycle and climate
136 changes. Finally, we present a protocol for implementing LULC in Earth System Model simulations
137 to be carried out in the current phase of the Palaeoclimate Modelling Intercomparison Project (PMIP:
138 Otto-Bleisner et al., 2017; Kageyama et al., 2018). However, the data sets and protocol will also be
139 useful in later phases of other CMIP projects, including the Land Use Model Intercomparison Project
140 (LUMIP) and the Land Surface, Snow and Soil Moisture Model Intercomparison Project (LS3MIP)
141 (Lawrence et al., 2016; van den Hurk et al., 2016).

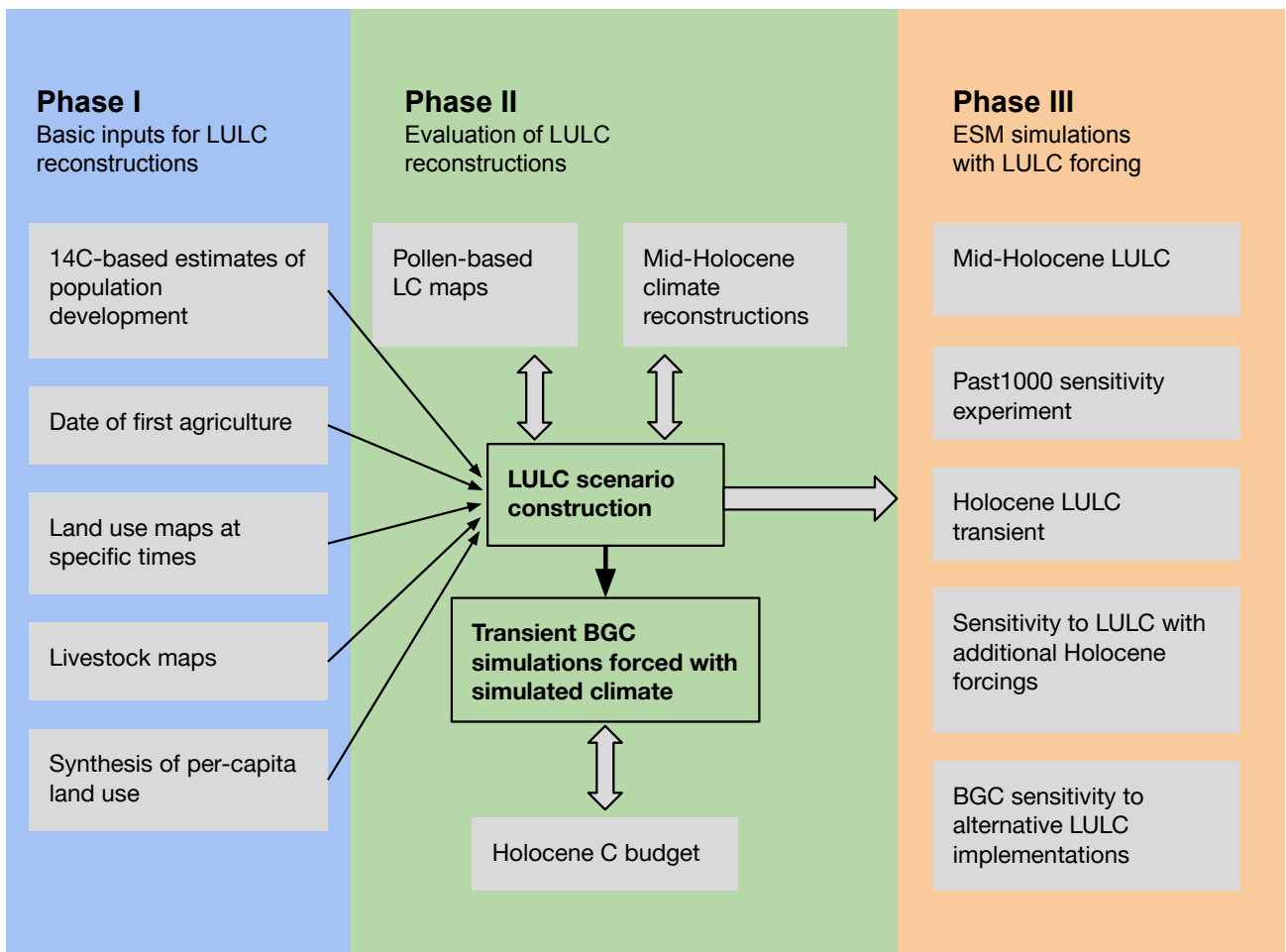
142
143

144 **2 LandCover6k Methodology**

145

146 The primary source of information about human exploitation of the landscape comes from
147 archaeological data. In general, these data are site specific and spatiotemporal coverage is often
148 patchy, and the types and quality of evidence available vary between sites and regions. Generalising
149 from site-specific data to landscape or regional scales involves making assumptions about human
150 behaviour and cultural practices. Because of the inherent uncertainties, we advocate an iterative
151 approach to incorporate archaeological data into LULC scenarios in LandCover6k (Fig. 2). We
152 propose to revise the existing LULC scenarios by incorporation of diverse archaeological inputs (Fig.
153 2, phase 1; see Sections 3 and 4) and to test the revised LULC scenarios for their plausibility and
154 consistency with other lines of evidence (Fig. 2, phase 2 with iterative testing; see Sections 5-7). As
155 a first test, the revised LULC scenarios of the extent of cropland and grazing land through time will
156 be compared with independent data on land-cover changes, specifically pollen-based reconstructions
157 of the extent of open land (see e.g. Trondman et al., 2015; Kaplan et al., 2017) (Section 5). Further
158 testing the LULC scenarios involves sensitivity tests using global climate models (Section 6) and
159 global carbon cycle models (Section 7). While the computational cost of the climate-model
160 simulations can be minimized using equilibrium time-slice simulations, the carbon cycle constraint
161 relies on transient simulations, but may be derived from uncoupled, land-only simulations. Simulated
162 climates at key times can be evaluated against reconstructions of climate variables (e.g. Bartlein et
163 al., 2011) (Section 6). The parallel evolution of CO₂ and its isotopic composition ($\delta^{13}\text{C}$) can be used
164 to derive the carbon balance of the terrestrial biosphere and the ocean separately (Elsig et al., 2009)
165 and, in combination with estimates for other contributors to land carbon changes such as C
166 sequestration by peat buildup, provides a strong constraint on the evolution of LULC through time.
167 An under- or over-prediction of anthropogenic LULC-related CO₂ emissions during a specific
168 interval results in consequences for the dynamics of the atmospheric greenhouse gas burden in

169 subsequent times (Stocker et al., 2017) (Section 7). Thus, these tests can be used to identify issues in
 170 the original archaeological datasets and/or the way these data were incorporated into the LULC
 171 scenarios that require further refinement. Phase 3 of the project (Fig. 2) provides a protocol for the
 172 implementation of the revised LULC scenarios in Earth System Model simulations (Section 8).
 173



174
 175 **Figure 2:** Proposed scheme for developing robust LULC scenarios through iterative testing and
 176 refinement, as input to Earth System Model (ESM) simulations. The archaeological inputs developed
 177 in Phase 1 can be used independently or together to improve the LULC reconstructions; iterative
 178 testing of the LULC scenario reconstruction (Phase 2) will ensure that these inputs are reliable before
 179 they are used of ESM simulations (Phase 3). The uppermost three LULC simulations capitalize on
 180 already planned baseline simulations without LULC; the lowermost two simulations are envisaged
 181 as new sensitivity experiments.
 182

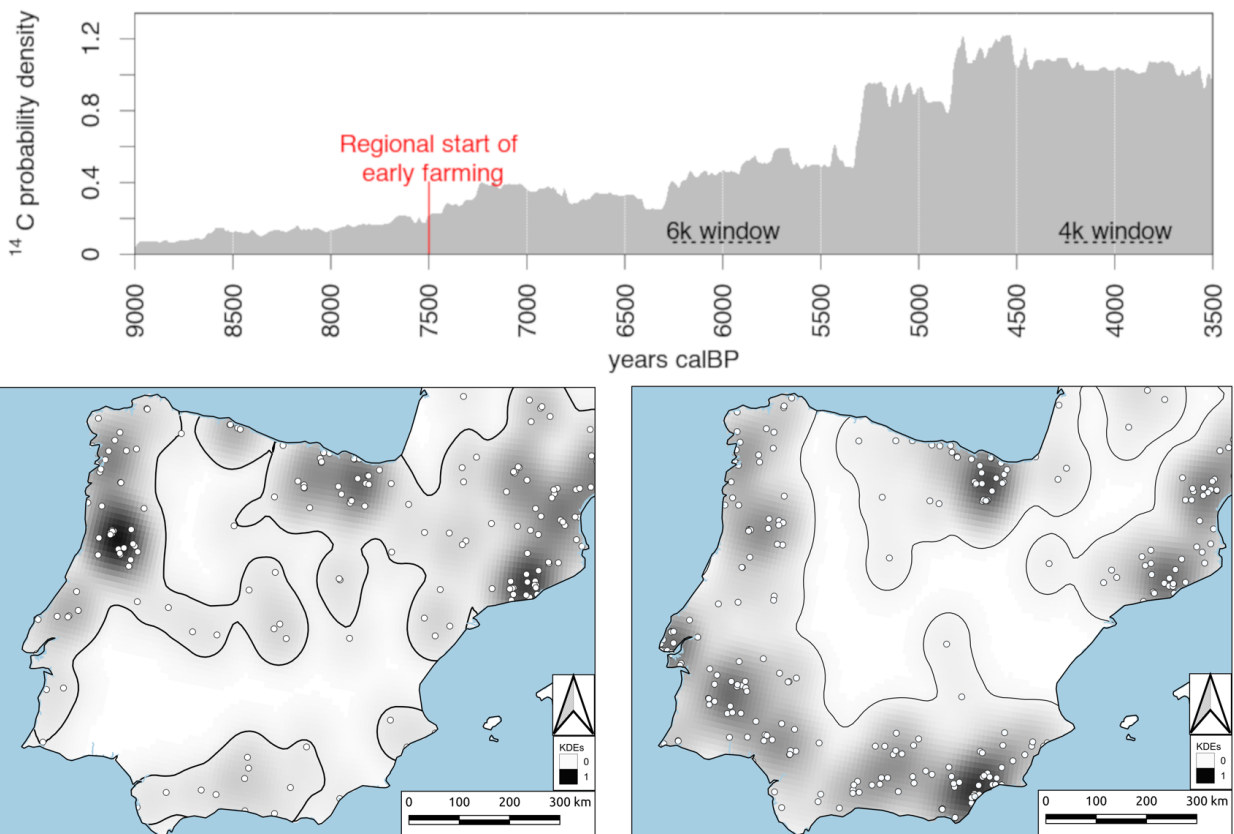
183 **3 Archaeological data inputs**
 184

185 LandCover6k is creating a number of products that will be used to improve the LULC scenarios
 186 (Figure 2). Here, we summarise the important features of these data products before showing how
 187 they will be incorporated within a scenario-development framework.
 188

189 **3.1 Population dynamics from ¹⁴C data**

190 Radiocarbon is the most routinely used absolute dating technique in archaeology, especially for the
 191 Holocene. Many thousands of radiocarbon dates are available from the archaeological literature. A
 192 number of regional and pan-regional initiatives are compiling these records through exhaustive
 193 survey of the archaeological literature (e.g. the Canadian Archaeological Radiocarbon Database:

194 <https://www.canadianarchaeology.ca/>). Statistical approaches, such as summed probability
 195 distributions (SPDs), can then be used to infer past demographic fluctuations from these compilations
 196 (Figure 3). This method assumes that the more people there were, the more remains of their various
 197 activities they left behind, and that this is directly reflected in the number of samples excavated and
 198 dated (Rick, 1987; Robinson et al., 2019). There are biases that could affect the expected one-to-one
 199 relationship between number of people and number of radiocarbon dates on archaeological material,
 200 including lack of uniform sampling through time and space caused by different archaeological
 201 research interests and traditions in different regions and increased preservation issues with increasing
 202 age, but these can be minimised through auditing the datasets. Assessment of the robustness of
 203 population reconstructions through time can be made statistically, by comparing a null hypothesis of
 204 demographic growth constructed from an exponential fit to the data with the actual record of number
 205 of dates through time (Shennan et al., 2013; Timpson et al., 2014). Mathematical simulations show
 206 that the method is relatively robust for large sample sizes (Williams, 2012). Radiocarbon dates have
 207 been successfully used in several regions to identify population fluctuations associated with hunter-
 208 gatherers (Japan: Crema et al., 2016) and the introduction of farming and subsequent changes in
 209 farming regimes (western Europe: Shennan et al., 2013; Wyoming: Zahid et al., 2016; South Korea:
 210 Oh et al., 2017; see also Freeman et al., 2018) as well as climatic oscillations (Ireland: Whitehouse et
 211 al., 2014).
 212



213
 214 **Figure 3:** Reconstruction of changes in population size in the Iberian Peninsula during the Holocene
 215 (9000 to 2000 BP, 9ka to 2ka BP) using summed probability distributions (SPDs) of radiocarbon
 216 dates (data after Balsera et al., 2015). The red line indicates the onset of agriculture in the region.
 217 The lower panels show areas under human use at 6ka (left) and 4ka (right) using kernel density
 218 estimates, where the white dots are actual archaeological sites and the shading shows the implied
 219 density of occupation.

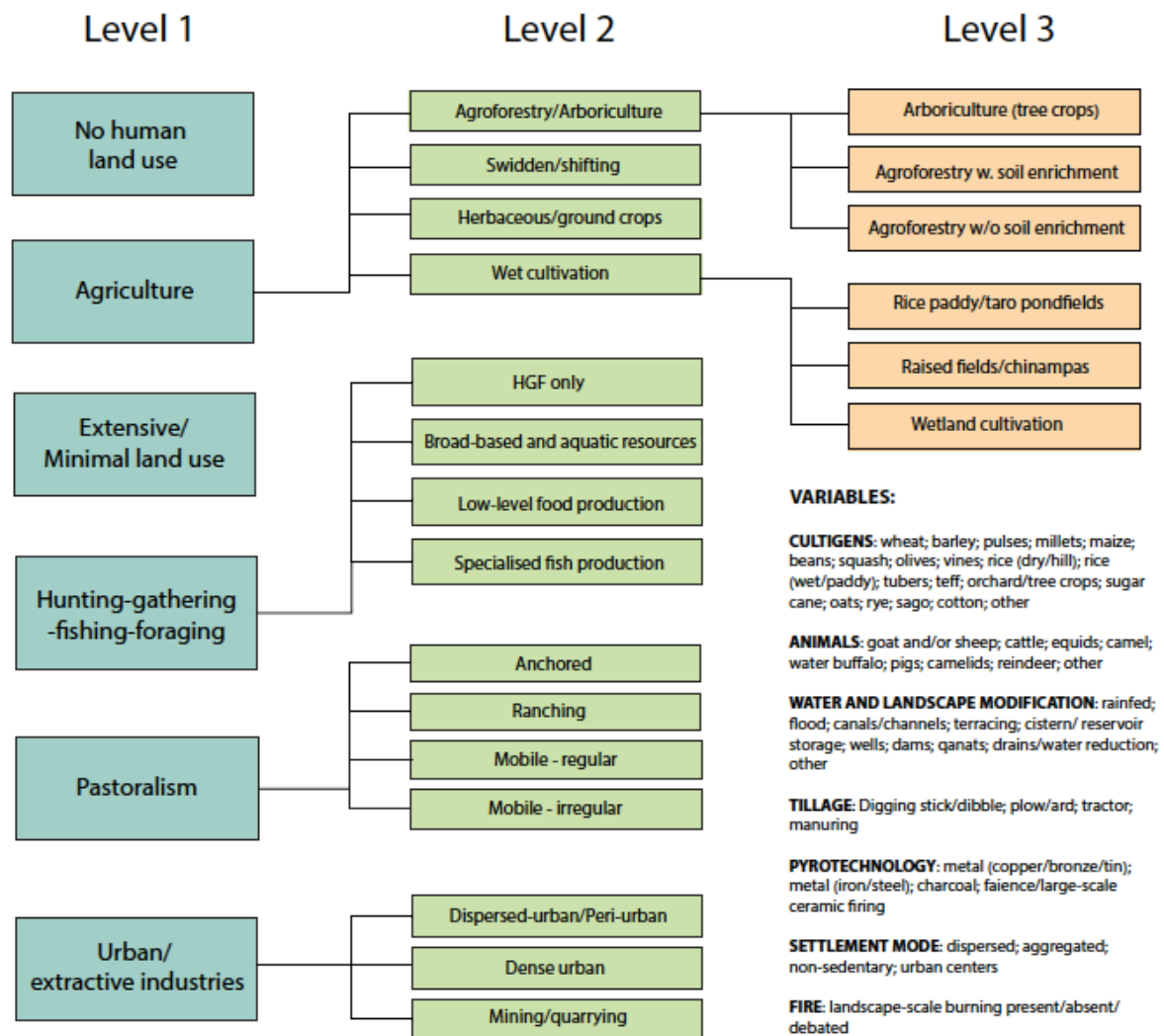
220
221
222
223
224
225
226
227
228
229
230
231
232
233
234
235
236
237
238
239
240
241
242
243
244
245
246
247
248
249
250

3.2 Date of first agriculture

Radiocarbon dates can also be used to track the timing and process of dispersal events, such as the diffusion of plant and animal domesticates from their initial centres of domestication. Since the distribution of samples is often patchy, geostatistical techniques such as kriging and splines are used to spatially interpolate the information in order to provide quantitative estimates of the timing of spread. Work carried out in Europe (Bocquet-Appel et al., 2009), Asia (Silva et al., 2015), and Africa (Russell et al., 2014) demonstrates that there are different rates of diffusion even within a region, reflecting the possible impact of natural features (e.g. waterways, elevation, ecology) on diffusion rates (Davison et al., 2006; Silva and Steele, 2014). Numerous studies provide robust local estimates for the earliest regional occurrence of agriculture and these are being synthesized to provide a global product within LandCover6k (Figure 2).

3.3 Global land-use and livestock maps

Maps of the distribution of archaeological sites or of areas linked to a given food production system have been produced for individual site catchments or small regions (e.g. Zimmermann et al., 2009; Barton et al., 2010; Kay et al., 2019). LandCover6k is developing global land-use maps for specific time windows, using a global hierarchical classification of land-use categories (Morrison et al., 2018) based on land-use types that are widely recognised from the archaeological record. At the highest level, the maps distinguish between areas where there is no (or only limited) evidence of land use, and areas characterized by hunting/foraging/fishing activities, pastoralism, agriculture, and urban/extractive land use (Fig. 4). Except in the cases where land use is minimal (no human land use, extensive/minimal land use), further distinctions are subsequently made to encompass the diversity of land-use activities in each land-use type (Fig. 4). A third level of distinction is made in the case of two categories (agroforestry, wet cultivation) where there are very different levels of intervention in different regions. Explanations of this terminology are given in Morrison et al. (2018). The LandCover6k land-use maps (see e.g. Fig. 5) will be based on different methods ranging from kernel-density estimates to expert assessments depending on the quality and quantity of the archaeological information available from different regions.



251
252
253
254

Figure 4: The hierarchical scheme of land-use classes used for global mapping in LandCover6k (updated from Morrison et al., 2018).

255
256
257
258
259
260
261
262
263
264

There is considerable variation in how intensely land is used both for crops and for grazing within broad land-use categories both geographically and through time (Ford and Clarke, 2015; Styring et al., 2017). Maps of land-use types do not provide direct information on the intensity of farming practices or how they translate into per-capita land use. Archaeological data about agricultural yields, combined with information from analogous contemporary cultures, historical information (e.g. Pongratz et al., 2008) and theoretical estimates of land use required to meet dietary and energy requirements (e.g. Hughes et al., 2018), can be used to provide regional estimates of per-capita land use for specific land-use categories. LandCover6k will synthesise this information to allow regionally specific estimates of per-capita land use to be derived from the global land-use maps.

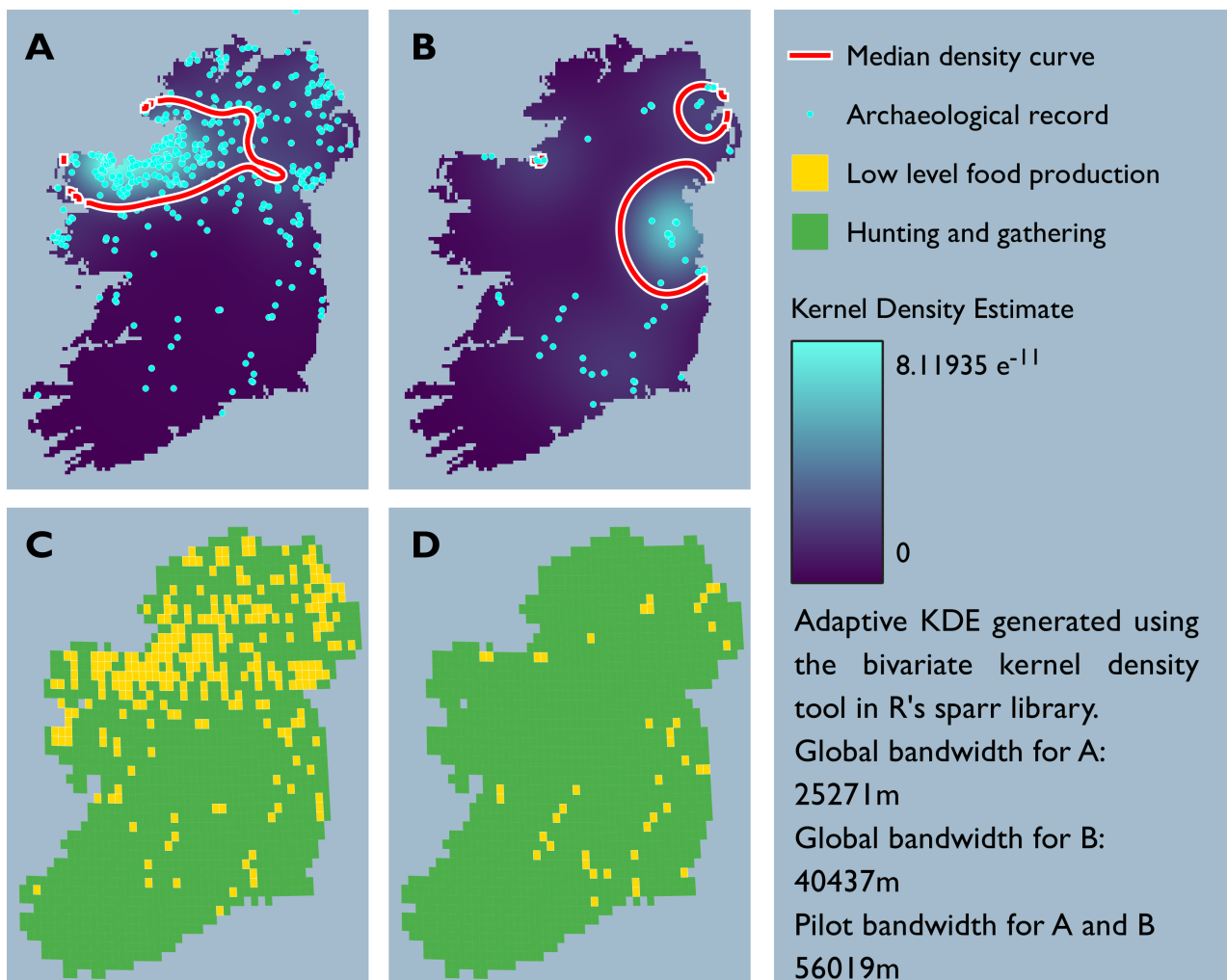
265
266
267
268
269
270
271

Information about the extent of grazing land is an important input for the development of revised LULC scenarios but, from a carbon-cycle modelling perspective, the amount of biomass removed by grazing is also a key parameter. Biomass loss varies not only with population size but also with the type of animal being reared (Herrero et al., 2013; Phelps & Kaplan, 2017) and thus information about what animals were present at a given location and estimates of population sizes are needed for improving the existing LULC scenarios. Although the conditions of bone preservation vary across the globe due to factors such as soil acidity, animal bones are routinely excavated (Lyman, 2008;

272 Reitz & Wing, 2008). Morphometric analysis of bones, along with collateral information such as age-
 273 related culling patterns, make it possible to determine whether these are the remains of domesticated
 274 species. We thus have a relatively precise idea of when livestock were introduced into a region, what
 275 types of animal were being reared at a given time, and can also make informed estimates of population
 276 size. Although the level of detail will vary geographically, this information can be used to produce
 277 global livestock maps.

278
 279 The harvesting of wood for domestic fires, building, and for industrial activities such as
 280 transportation, pottery-making and metallurgy is an important aspect of human exploitation of the
 281 landscape in the pre-industrial period (McGrath et al., 2015). It has been argued that even Mesolithic
 282 hunter-gatherer communities shaped their environment through wood harvesting (Bishop et al.,
 283 2015). Approaches have been developed to quantifying the wood harvest associated with
 284 archaeological settlements at specific times based on the evidence of types of wood use, household
 285 energy requirements, population size, and calorific value of the wood used (see e.g. Marston, 2009;
 286 Janssen et al., 2017). However, quantitative information on ancient technology and lifestyle is sparse
 287 and direct estimates of the amount of wood harvest through time are likely to remain highly uncertain
 288 (Marston et al., 2017; Veal, 2017). Nevertheless, combining evidence-based inferential approaches
 289 with improved estimates of population size should allow changes in wood harvesting to be taken into
 290 account in constructing revised LULC scenarios.

291



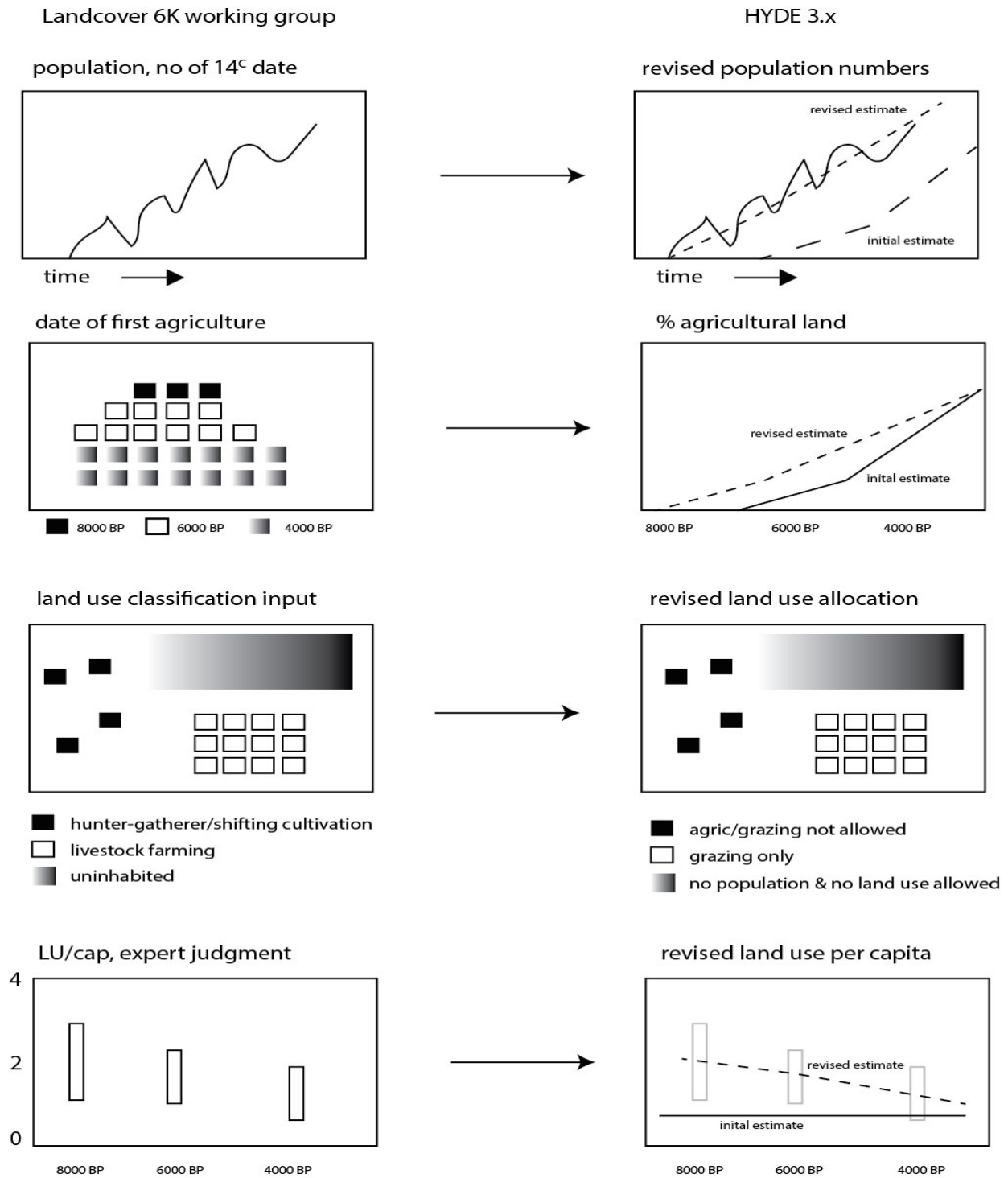
292
 293 **Figure 5:** An example of regional land-use mapping. The upper panels show the distribution of known
 294 archaeological sites superimposed on kernel density estimates of the extent of land-use based on the
 295 density of observations, and the lower panels show these data superimposed on the LandCover6k

296 *land-use classes for the Middle Neolithic (3600-3400 years BCE, 5600-5400 years BP, 5.6-5.4 ka*
297 *BP) (left panels) and the Early Neolithic (3750-3600 years BCE, 5750-5600 years BP, 5.7-5.6 ka BP)*
298 *(right panels) of Ireland. Data points derive from ¹⁴C dated archaeological sites and distributions of*
299 *settlements and monuments that have been assigned to each archaeological period following the*
300 *dataset published in McLaughlin et al. (2016). The assigned land-use classes are inferred from*
301 *archaeological material from one (or more) sites within the grid box. It should not be assumed that*
302 *the whole gridcell was being used for agriculture during the Middle and Early Neolithic. Informed*
303 *assessment suggests that agricultural land (crop growing and grazing combined) probably occupied*
304 *between 10-15% of the total grid area in the low-level food production regions of the eastern and*
305 *western coastal areas, whilst agricultural land likely represents 5% or less of the total grid cell area*
306 *in inland areas.*
307

308 **4. Incorporation of archaeological data in LULC scenarios**

309
310 The existing LULC scenarios are substantially dependent on historical regional population estimates
311 at key times, which are then linearly interpolated to provide a year-by-year estimate of population.
312 Estimates of regional population growth based on suitably screened ¹⁴C data can be used to modify
313 existing population growth curves (Figure 6), both in terms of establishing the initial date of human
314 presence and by modifying a linear growth curve to allow for intervals of population growth and
315 decline.
316

317 Information on the timing of the first appearance of agriculture at specific locations can be used to
318 constrain the temporal record of LULC changes in the scenarios. This information can also be used
319 to allocate LULC changes geographically across regions (Figure 6). Global land-use maps can be
320 used to identify areas where there was no permanent agricultural activity at a given time (e.g. either
321 unsettled areas or areas occupied by hunter-gatherer communities) and provide a further constraint
322 on the geographic extent of the LULC changes given by the scenarios (Figure 6). The type of
323 agriculture, including whether the region was predominantly used for tree or annual crops or for
324 pasture, modifies the area of open land specified in the LULC scenarios. Information on the extent of
325 rain-fed versus irrigated agriculture, as indicated by the presence of irrigation structures associated
326 with archaeological sites, can also be used to refine the distribution of these classes in the LULC
327 scenarios. Per-capita land-use estimates and their changes through time (see e.g. Hughes et al., 2018;
328 Weiberg et al., 2019) provide a further refinement of the LULC scenarios, allowing a better
329 characterization of the distinction between e.g. areas given over to extensive versus intensive animal
330 production (rangeland versus pasture in the HYDE 3.2 terminology). There will remain areas of the
331 world for which this kind of fine-grained information is not available. Nevertheless, by incorporating
332 information where this exists, the LandCover6k products will contribute to a systematic refinement
333 of existing LULC scenarios. Iterative testing of the revised scenarios will ensure that they are robust.
334



335
 336 **Figure 6:** Schematic illustration of the proposed implementation of ¹⁴C-based population estimates,
 337 date of first agriculture, land-use maps, and land-use per capita information in the HYDE model
 338 (here indicated as HYDE3.x). The archaeological data are represented as values for a grid cell in
 339 geographic space at a given time for date of first agriculture and land use, but as a time series for a
 340 specific grid cell for population and land-use per capita. In the case of population estimates, date of
 341 first agriculture and land-use per capita data, we show the initial estimate and the revised estimate
 342 after taking the archaeological information into account in the HYDE3.x plot. It should be assumed
 343 in the case of the land-use mapping that the original estimate was that there was no land use in this
 344 region.
 345

346
347
348
349
350
351
352
353
354
355
356
357
358
359
360
361
362
363
364
365
366
367
368
369
370
371
372
373
374
375
376
377
378
379
380
381
382
383
384
385
386
387
388
389
390
391
392
393
394
395

5. Using pollen-based reconstructions of land cover changes to evaluate LULC scenarios

Pollen-based vegetation reconstructions can be used to corroborate archaeological information on the date of first agriculture from the appearance of cereals and agricultural weeds. These reconstructions can also be used to test the LULC reconstructions, either using relative changes in forest cover or reconstructions of the area occupied by different land cover types. LandCover6k uses the REVEALS pollen source-area model (Sugita, 2007) to estimate vegetation cover from fossil pollen assemblages. REVEALS predicts the relationship between pollen deposition in large lakes and the abundance of individual plant taxa in the surrounding vegetation at a large spatial scale (ca. 100 km x 100 km; Hellman et al., 2008a, b) using models of pollen dispersal and deposition. REVEALS can also be used with pollen records from multiple small lakes or peat bogs (Trondman et al., 2016) although this results in larger uncertainties in the estimated area occupied by individual taxa. The estimates obtained for individual taxa are summed to produce estimates of the area occupied by either plant functional (e.g. summer-green trees, evergreen trees) or land cover (e.g. open land, grazing land, cropland) types.

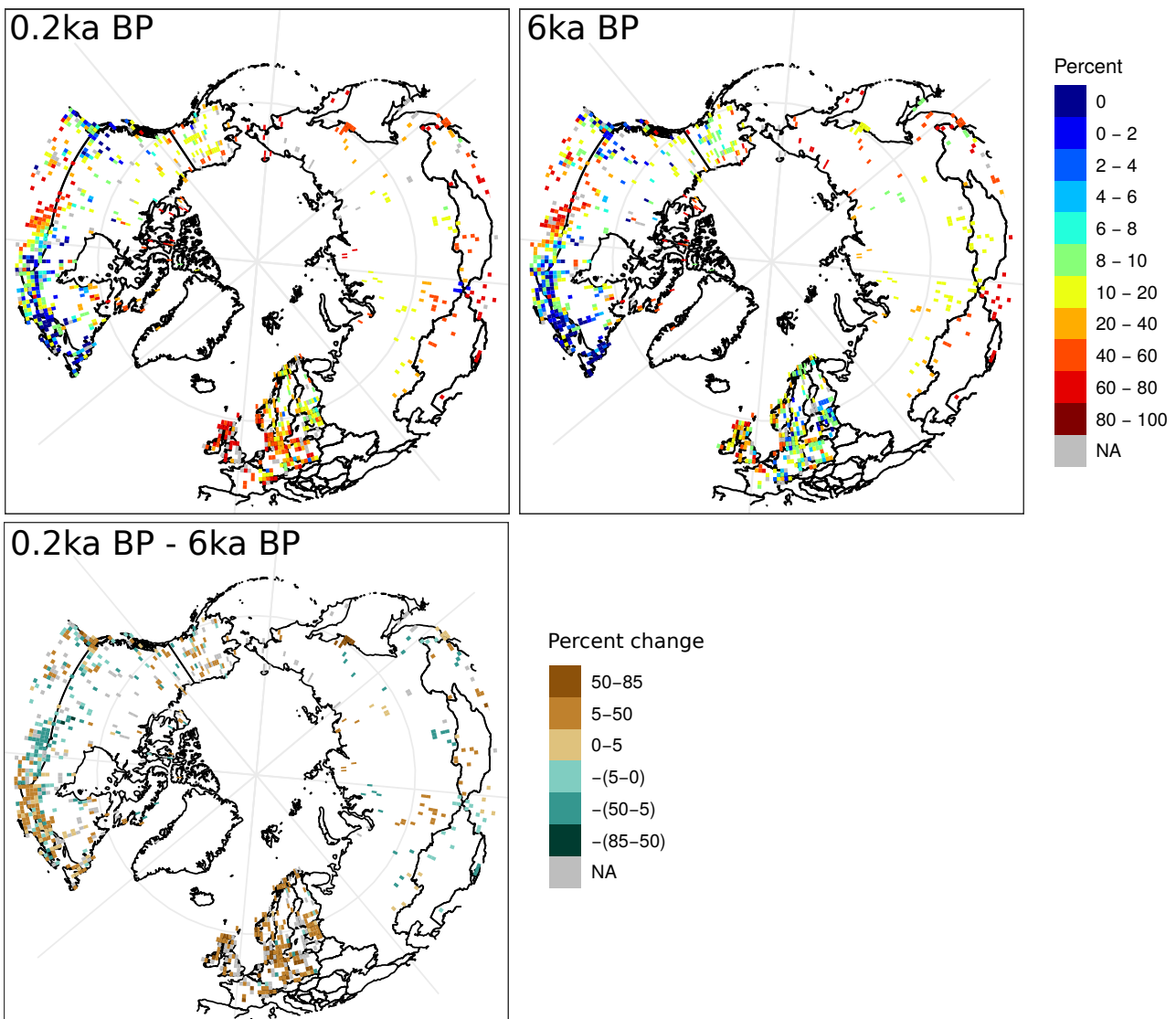
The geographic distribution of pollen records is uneven. There are also many areas of the world where environments that preserve pollen (i.e. lakes, bogs, forest hollows) are sparse. Site-based reconstructions of land cover are therefore interpolated statistically to produce spatially continuous reconstructions (Nielsen et al., 2012; Pirzamanbein et al., 2014; Pirzamanbein et al., 2018). LandCover6k uses a 1° resolution grid and all available pollen records in each grid cell to produce an estimate of land cover per grid cell through time. The more pollen records per grid cell and pollen counts per time window, the smaller the estimated error on the land-cover reconstruction. The uncertainties on the pollen-based REVEALS reconstructions are partly expressed by their standard errors (SEs). These SEs take into account the SE on the relative pollen productivity (RPP) of each plant taxon included in the REVEALS reconstructions and the variability between the site-specific REVEALS reconstructions (e.g. Trondman et al., 2015). The uncertainties on the pollen-based land cover reconstructions are taken into account when these reconstructions are compared with LULC scenarios (Kaplan et al., 2017).

The REVEALS approach has already been used to produce gridded reconstructions of changes in the amount of open land through time across the northern extratropics (Figure 7; Dawson et al., 2018). These reconstructions provide mean plant cover for time slices of 500 years through the Holocene until 0.7ka BP, and three historical time windows (modern–0.1ka BP, 0.1–0.35ka BP, and 0.35–0.7ka BP). The more pollen samples per time interval and pollen records per grid cell, the more years within the 500 yrs time slice will be represented in the reconstruction. This implies that the number of years represented in a time-slice reconstruction varies in space and time.

A major limitation in applying REVEALS globally is the requirement for information about the relative pollen productivity (RPP) of individual pollen taxa, which is currently largely lacking for the tropics. However, LandCover6k has been collecting RPPs for China, South-East India, Cameroon, Brazil and Argentina and pollen-based land-cover reconstructions will be available for sufficient parts of the tropics to allow testing of the LULC scenarios. Another limitation of the REVEALS reconstructions is that RPP estimates are available for cultivated cereals but not for other cultivars or cropland weeds, so the LandCover6k pollen-based reconstructions will generally underestimate cropland cover (Trondman et al., 2015). It may also be possible to use alternative pollen-based reconstructions of land cover changes, such as the Modern Analogue Approach (MAT: e.g. Tarasov et al., 2007; Zanon et al. 2018); pseudo-biomization (e.g. Fyfe et al., 2014) or STEPPS (Dawson et

396 al., 2016). While none of these methods require RPPs, MAT and STEPPS can only be applied in
 397 regions where the pollen datasets have dense coverage (such as Europe and North America) and
 398 pseudo-biomization is affected by the non-linearity of the pollen-vegetation relationship that the
 399 REVEALS approach is designed to remove.

400
 401 Comparison of the reconstructions of the extent of open land with the LULC deforestation scenarios
 402 will provide a first evaluation of the realism of the revised LULC scenarios (e.g. Kaplan et al., 2017).
 403 Underestimation or overestimation of open land in the LULC scenarios is not necessarily an
 404 indication that these scenarios are inaccurate because (a) pollen-based reconstructions cannot
 405 distinguish between anthropogenic and climatically determined natural open land (e.g. natural
 406 grasslands, steppes, wetlands) and (b) REVEALS underestimates cropland cover because there are
 407 no RPP estimates for cultivars other than cereals. However, overestimation of the area of open land
 408 in the LULC scenarios might suggest problems either in the archaeological inputs or their
 409 implementation, especially for times or regions when other evidence indicates cereals were the major
 410 crop. In this sense, despite potential problems, the LandCover6k pollen-based reconstructions of land
 411 cover will provide an important independent test of the revised LULC scenarios.
 412



413
 414
 415 **Figure 7:** Northern extratropical (>40°N) mean fractional cover of open land at 6000 years ago (6ka
 416 BP: top right panel) and 200 years ago (0.2ka BP: top left panel) estimated using REVEALS, and the

417 difference in fractional cover between the two periods (lower panel), where red indicates an increase
418 in open land and blue a decrease (after Dawson et al., 2018).

419

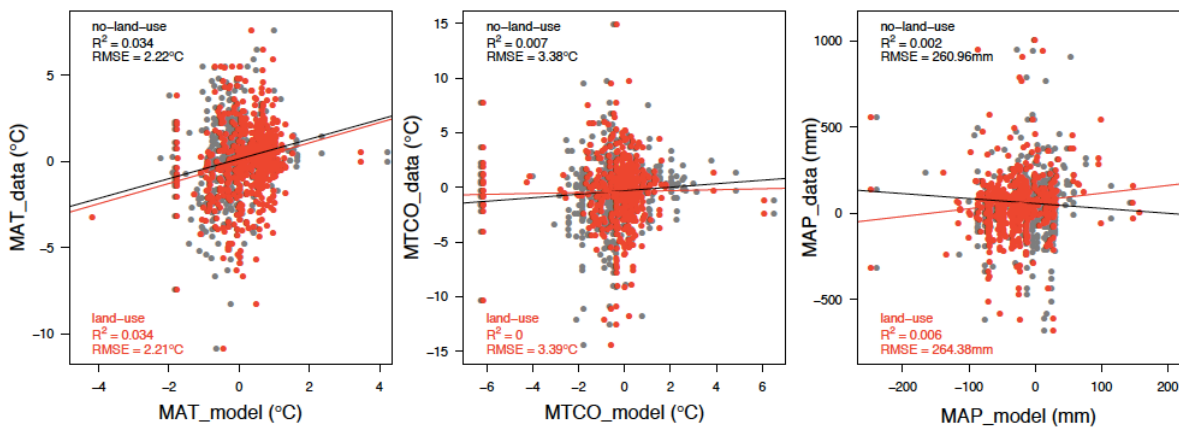
420

421 6. Testing the reliability of improved scenarios using climate-model simulations

422

423

424 A second test of the realism of the improved LULC scenarios is to examine whether incorporating
425 LULC changes improves the realism of the simulated climate when compared to palaeoclimate
426 reconstructions (Figure 8). The mid-Holocene (6000 years ago, 6 ka BP) is an ideal candidate for
427 such a test because benchmark data sets of quantitative climate reconstructions are available (e.g.
428 Bartlein et al., 2011), the interval has been a focus through multiple phases of PMIP, control
429 simulations with no LULC have already been run, and evaluation of these simulations has identified
430 regions where there are major discrepancies between simulated and reconstructed climates e.g. the
431 observed expansion of northern hemisphere monsoons, climate changes over Europe, the magnitude
432 of high-latitude warming, and wetter conditions in central Eurasia (Mauri et al., 2014; Harrison et al.,
433 2015; Bartlein et al., 2017). There are discernible anthropogenic impacts on the landscape in many
434 of these regions by 6 ka, although they are not as strong as during the later Holocene and they are not
435 present everywhere. Nevertheless, the 6ka BP interval provides a good focus for testing whether
436 improvements to the LULC scenarios produces more realistic simulations of climate. Such an
437 evaluation would need to go beyond the global comparison made here (Figure 8) to regional
438 comparisons to identify whether improvements in simulated climate in regions where there is a large
439 anthropogenic impact on land cover do not result in a degradation in the simulated climate elsewhere.
440



441

442

443 **Figure 8:** Quantitative comparison of the change in climate between the mid-Holocene (6ka) and the
444 pre-industrial period as shown by pollen-based reconstructions gridded to $2 \times 2^\circ$ resolution to be
445 compatible with the model resolution (from Bartlein et al., 2011) and in simulations with and without
446 the incorporation of land-use change (from Smith et al., 2016). This figure illustrates the approach
447 that will be taken to evaluate the impact of new LULC scenarios on climate. The imposed land-use
448 changes at 6000 years ago (6ka BP) were derived from the KK10 scenario (Kaplan et al., 2011). The
449 plots show comparisons of mean annual temperature (MAT), mean temperature of the coldest month
450 (MTCO) and mean annual precipitation (MAP) for the northern extratropics (north of 30° N), where
451 each dot represents a model grid cell where comparisons with the pollen-based reconstructions is
452 possible. Although the incorporation of land use produces somewhat warmer and wetter climates in
453 these simulations, overall the incorporation of land-use produces no improvement of the simulated
454 climates at sites with pollen-based reconstructions.

455

456 **7. Testing the reliability of improved scenarios using carbon-cycle models**

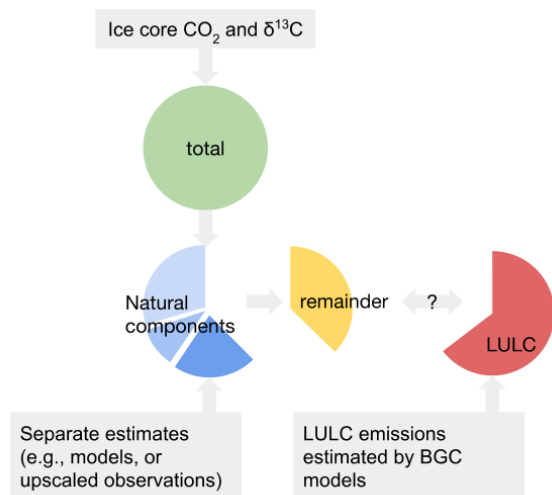
457

458 Carbon-cycle modelling will be used as a further test of the realism of the improved LULC scenarios.
459 Two constraints are available for testing the realism of past LULC scenarios. First, reconstructions
460 of LULC history must converge on the present-day state, which is relatively well constrained by
461 satellite land-cover observations and national statistics on the amount of land under use.
462 Reconstructing the extent of past LULC change thus reduces to allocating a fixed total amount of
463 land conversion from natural to agricultural use over time. More conversion in earlier periods implies
464 less conversion in later periods. At the continental to global scale, cumulative LULC emissions scale
465 linearly with the agricultural area. LULC scenarios that converge to the present-day state also
466 converge to within a small range of cumulative historical emissions (Stocker et al., 2011; Stocker et
467 al., 2017). Deviations from a linear relationship between extent and emissions are due to differences
468 in biomass density in potential natural and agricultural vegetation of different regions affected by
469 anthropogenic LULC. Differences in cumulative emissions for alternative LULC reconstructions
470 with an identical present-day state are due to the long response time of soil carbon content following
471 a change in carbon inputs and soil cultivation. Conserving the total extent of LULC (and allocating a
472 fixed total expansion over time) is thus approximately equivalent to conserving cumulative historical
473 LULC emissions. Thus, more LULC CO₂ emissions in earlier periods imply less CO₂ emissions in
474 more recent periods.

475

476 The total C budget of the terrestrial biosphere provides a second constraint on LULC emissions
477 through time. The net C balance of the land biosphere, which reflects the sum of all natural and
478 anthropogenic effects on terrestrial C storage, can be reconstructed from ice-core data of past CO₂
479 concentrations and $\delta^{13}\text{C}$ composition (Elsig et al. 2009). Providing that all of the natural contributions
480 to the land C inventory (e.g. the build-up of natural peatlands: Loisel et al., 2014) can be specified
481 from independent evidence, the anthropogenic sources can be estimated as the difference between the
482 total terrestrial C budget and natural contributions (Figure 9) at any specific time.

483



484

485 **Figure 9:** Illustration of the terrestrial C budget approach to evaluate LULC. The total terrestrial C
486 balance (green circle 'total') is constrained by ice core records of CO₂ and its isotopic signature
487 ($\delta^{13}\text{C}$). Estimates for C balance changes of different natural land carbon cycle components (e.g.,
488 peatlands, permafrost, forest expansion/retreat, desert greening) can be estimated independently
489 (blue slices 'Natural components') either from empirical upscaling of site-scale observations or from
490 model-based analyses (BGC models forced with varying climate). The remainder (yellow slice
491 'remainder') is then calculated as the total terrestrial C balance (green circle 'total') minus the sum
492 of the separate estimates of the natural components (blue slices 'Natural components'). The remainder

493 *is effectively the emissions resulting from LULC changes, and can therefore be compared to LULC*
 494 *CO₂ emission estimates by carbon-cycle models.*

495
 496 Transient simulations with a model that simulates CO₂ emissions in response to anthropogenic LULC
 497 can be used to test the reliability of the LULC scenarios, by comparing results obtained with
 498 prescribed LULC changes through time against a baseline simulation without imposed LULC. This
 499 will necessitate making informed decisions about the fraction of land under cultivation that is
 500 abandoned or left fallow each year, and the maximum extent of land affected by such episodic
 501 cultivation. We envisage using several different offline carbon-cycle models for this purpose in order
 502 to take account of uncertainties associated with differences between the carbon-cycle models. The
 503 carbon-cycle simulations will be driven by climate outputs (temperature, precipitation and cloud
 504 cover) from an existing transient climate simulation made with the ECHAM model (Fischer and
 505 Jungclaus, 2011) and CO₂ prescribed from ice-core records. The CO₂ emission estimates from these
 506 two simulations will then be evaluated using C budget constraints. This evaluation will allow us to
 507 pinpoint potential discrepancies between known terrestrial C balance changes and estimated LULC
 508 CO₂ emission in given periods over the Holocene.

511 **8. Implementation of LULC in Earth System Model simulations**

512
 513 We propose a series of simulations to examine the impact of LULC, using the revised LULC scenarios
 514 from LandCover6k and building on climate-model experiments that are currently being run either in
 515 CMIP6-PMIP4 (*midHolocene, past1000*) or within PMIP although not formally included as CMIP6-
 516 PMIP4 experiments.

517
 518 The *mid-Holocene* (and its corresponding *piControl*) simulation is one of the PMIP entry cards in the
 519 CMIP6-PMIP4 experiments (Kageyama et al., 2018; Otto-Bliesner et al., 2017) and it is therefore
 520 logical to propose this period for LULC simulations. The LULC sensitivity experiment
 521 (*midHoloceneLULC*) should therefore follow the CMIP6-PMIP4 protocol, that is it should be run
 522 with the same climate-model components and following the same protocols for implementing
 523 external forcings as used in the two CMIP6-PMIP4 experiments (Table 1). Thus, if the *piControl* and
 524 *midHolocene* simulations are run with interactive (dynamic) vegetation, then the *midHoloceneLULC*
 525 experiment should also be run with dynamic vegetation in regions where there is no LULC change.
 526 For most models, this means that the LULC forcing is imposed as a fraction of the grid cell and the
 527 remaining fraction of the grid cell has simulated natural vegetation. These new mid-Holocene
 528 simulations would allow for a better understanding of the relationship between climate changes and
 529 land-surface feedbacks (including snow albedo feedbacks), and the role of water recycling at a
 530 regional scale. Thus, modelling groups who are running the *midHolocene* experiment with a fully
 531 interactive carbon cycle could also run the LULC experiment allowing atmospheric CO₂ to evolve
 532 interactively, subject to the simulated ocean and land C balance.

533
 534 **Table 1:** Boundary conditions for CMIP6-PMIP4 and the mid-Holocene LULC experiments. The
 535 boundary conditions for the CMIP6-PMIP4 *piControl* and *midHolocene* are described in Otto-
 536 Bleisner et al. (2017) and are given here for completeness.

Boundary conditions		1850CE (DECK <i>piControl</i>)	6ka (<i>midHolocene</i>)	6ka LULC (<i>midHoloceneLULC</i>)
Orbital parameters	Eccentricity	0.016764	0.018682	0.018682
	Obliquity	23.459	24.105	24.105

	Perihelion – 180	100.33	0.87	0.87
	Vernal equinox	Noon, 21 March	Noon, 21 March	Noon, 21 March
Greenhouse gases	Carbon dioxide (ppm)	284.3	264.4	264.4
	Methane (ppb)	808.2	597.0	597.0
	Nitrous oxide (ppb)	273.0	262.0	262.0
	Other GHG	DECK <i>piControl</i>	0	0
Other boundary conditions	Solar constant	TSI: 1360.747	As <i>piControl</i>	As <i>piControl</i>
	Palaeogeography	Modern	As <i>piControl</i>	As <i>piControl</i>
	Ice sheets	Modern	As <i>piControl</i>	As <i>piControl</i>
	Vegetation	Interactive	Interactive	pasture and crop distribution prescribed from a revised scenario
		DECK <i>piControl</i>	As <i>piControl</i>	pasture and crop distribution prescribed from a revised scenario
	Aerosols	interactive	Interactive	Interactive
DECK <i>piControl</i>		As <i>piControl</i>	As <i>piControl</i>	

538

539

540

541

542

543

544

545

546

547

548

549

550

551

552

553

554

555

556

557

558

559

560

561

562

563

The real strength of the revised LULC scenarios is to provide boundary conditions for transient climate-model simulations. The CMIP6-PMIP4 simulation of 850-1850 CE (*past1000*) already incorporates LULC changes as a forcing (Jungclaus et al. 2017), based on a harmonized data set that provides LULC changes from 850 through to 2015 CE (Hurtt et al., 2017), which in turn draws on output from the HYDE3.2 scenario (Klein Goldewijk et al., 2017a). The *past1000* protocol (Jungclaus et al., 2017) acknowledges that this default land-use data set is at the lower end of the spread in estimates of early agricultural area indicated by other LULC scenarios and recommends that modelling groups run additional sensitivity experiments using alternative maximum and minimum scenarios. The revised LULC scenarios created by LandCover6k could be used as an alternative to these maximum and minimum scenarios. Other than the substitution of the LandCover6k scenario, the specifications of other forcings would then follow the recommendations for the CMIP6-PMIP4 *past1000* simulation.

A transient climate simulation for a longer period of the Holocene would provide a more stringent test of the impact of LULC on the coupled earth system. We suggest that this transient simulation (*holotrans*) should start from the pre-existing *midHolocene* simulation to capitalise on the fact that the *midHolocene* simulation has been spun up for sufficiently long (Otto-Bleisner et al., 2017) to ensure that the ocean and land carbon cycle is in equilibrium at the start of the transient experiment (Table 2). In order to be consistent with the CMIP6-PMIP4 *midHolocene* protocol (Otto-Bleisner et al., 2017), changes in orbital forcing should be specified from Berger and Loutre (1991) and year-by-year changes in CO₂, CH₄ and N₂O should be specified following Joos and Spahni (2008). LULC changes should be implemented by imposing crop and pasture area through time as specified in the revised LULC scenarios; elsewhere, the simulated vegetation should be active. It will be necessary

564 to run the Holocene transient climate simulation in two steps. A first simulation (*holotrans_LULC*)
 565 should be run using prescribed atmospheric CO₂ concentration even though the carbon cycle is fully
 566 interactive, because this will establish the consistency of the carbon cycle in the land surface model.
 567 However, once this is done it will be possible to re-run the simulations with interactive CO₂
 568 emissions. Table 3 provides a summary of the proposed ESM simulations.

570 **Table 2:** Boundary conditions for baseline PMIP Holocene transient (6 ka BP to 1850 CE) and LULC
 571 transient simulations

		Mode	Source/Value	LULC experiment
Orbital parameters		transient		As baseline simulation
Greenhouse gases	CO ₂	transient	Dome C	As baseline simulation
	CH ₄		Combined EPICA & GISP record	As baseline simulation
	N ₂ O		Combined EPICA NGRIP, & TALDICE record	As baseline simulation
Solar forcing		transient	Steinhilber et al. (2012)	As baseline simulation
Volcanic forcing		transient	To be determined	As baseline simulation
Palaeogeography		Constant at PI values	Modern	As baseline simulation
Ice sheets		Constant at PI values	Modern	As baseline simulation
Vegetation		interactive		LC6k transient pasture and crop distribution imposed
Aerosols		Constant at PI values		As baseline simulation

572
 573
 574 Unlike the situation for the mid-Holocene, where there is a global climate benchmark data set
 575 (Bartlein et al., 2011) which provides reconstructions of multiple bioclimatic variables of seasonal
 576 temperature and moisture, the opportunities for quantitative evaluation of the *holotrans* simulated
 577 climate are more limited. Seasonal temperature reconstructions are available for Europe (Davis et
 578 al., 2003) and North America (Viau et al, 2006; Viau and Gajewski, 2009). Although there is a new
 579 global data set that provides global temperature reconstructions for the Holocene (Kaufman et al., in
 580 press), it is based on only 472 terrestrial records worldwide and the results for zonally averaged
 581 temperature changes are therefore likely to be more robust than the regional details. There are also
 582 time series reconstructions for individual sites outside these two regions (e.g. Nakagawa et al.,
 583 2002; Wilmshurst et al., 2007; Ortega-Rosas et al., 2008). Furthermore, the simulated time-course
 584 of CO₂ emissions can be compared to the ice core records.

585
 586 **Table 3:** Summary of proposed simulations.

Name	Mode	Purpose
<i>piControl</i>	equilibrium	Standard CMIP6-PMIP4 simulation

<i>midHolocene</i>	equilibrium	Standard CMIP6-PMIP4 simulation
<i>midHoloceneLULC</i>	equilibrium	Sensitivity to LULC changes
<i>holotrans</i>	transient	Baseline fully transient simulation from 6ka onwards, with no LULC
<i>holotrans_LULC</i>	transient	Fully transient simulation from 6ka onwards, with LULC imposed

587

588

589

590

591

592

593

594

595

596

597

598

599

600

601

602

603

604

605

606

607

608

609

610

611

612

613

614

615

616

617

618

619

620

621

622

623

624

625

626

627

The CMIP6-PMIP4 *mid-Holocene* simulations are stylized experiments, lacking several potential forcings (in addition to LULC), including changes in atmospheric dust loading, in solar irradiance, and volcanic forcing. We suggest that additional sensitivity tests could be run to take these additional forcings into account. In the case of solar and volcanic forcing, this would also ensure that the transient *holotrans* simulations mesh seamlessly with the *past1000* simulation. Changes in solar variability during the Holocene should be specified from Steinhilber et al. (2012). There are records of volcanic forcing for the past 2000 years (Sigl et al., 2015; Toohey and Sigl, 2017), and these are used in the *past1000* simulation. Observationally constrained estimates of the volcanic stratospheric aerosol for Holocene are currently under development (M. Sigl, pers comm.) and could be implemented as an additional sensitivity experiment when available. Changes in atmospheric dust loading are not included in the *past1000* simulation but are important during the earlier part of the Holocene (Pausata et al., 2016; Tierney et al., 2017; Messori et al., 2019). Although continuous reconstructions of dust loading through the Holocene are not available, it would be possible to use estimates for particular time-slices (Egerer et al., 2018) to test the sensitivity to this forcing.

Outcomes and Perspectives

LandCover6k has developed a scheme for using archaeological information to improve existing scenarios of LULC changes during the Holocene, specifically by using archaeological data to provide better estimates of regional population changes through time, better information on the date of initiation of agriculture in a region, more regionally specific information about the type of land use, and more nuanced information about land-use per capita than currently implemented in the LULC scenarios generated by HYDE and KK10. While the final global data set are still in production, fast-track priority products have been created and their impact on current scenarios is being tested.

Although the work of LandCover6k will provide more solid knowledge about anthropogenic modification of the landscape, some information will inevitably be missing and some key regions will be poorly covered. There will still be large uncertainties associated with revised LULC scenarios, even though these will be based on more solid evidence than the existing LULC scenarios. Documenting the uncertainties in the archaeological inputs and their impacts on the revised scenarios is an important goal of the LandCover6k project. We propose using the information about the uncertainties in the archaeological data sources to generate multiple LULC scenarios comparable to the "low-end", "high-end" scenarios used for e.g. in future projections. Furthermore, we have proposed a series of tests that will help to evaluate the realism of the final scenarios, based on independent evidence from pollen-based reconstructions of land cover, reconstructions of climate, and carbon-cycle constraints. These tests should help in identifying which of the potential LULC reconstructions are most realistic and in constraining the sources of uncertainty.

628 We have proposed the use of offline carbon-cycle simulations solely as a test of the realism of the
629 revised LULC scenarios. Quantifying the LULC contribution to CO₂ emissions during the Holocene
630 would require additional simulations in which other forcings (climate, atmospheric CO₂, insolation)
631 are kept constant. The difference in simulated total terrestrial C storage between these simulations
632 and LULC simulations provides an estimate of *primary emissions* (Pongratz et al., 2014) and avoids
633 additional model uncertainty regarding the sensitivity of land C storage to atmospheric CO₂ or climate
634 being included in emission estimates. There are other sensitivity tests that would be useful. For
635 example, vegetation-carbon-cycle models differ in their ability to account for gross land use
636 transitions within grid cells (Arneeth et al., 2017). This is critical for simulating effects of non-
637 permanent agriculture where land is simultaneously abandoned and re-claimed within the extent of a
638 model grid cell. Such shifting cultivation-type agriculture implies forest degradation in areas
639 recovering from previous land use and leads to substantially higher LULC emissions compared to
640 model estimates where only net land-use changes are accounted for (Shevliakova et al., 2009). It
641 would therefore be interesting to run additional simulations accounting for net land use change, and
642 indeed separating out the effects of wood harvesting and shifting cultivation.
643

644 We anticipate that it will be possible to incorporate realistic LULC scenarios for the mid-Holocene
645 as part of the climate-model sensitivity experiments planned during PMIP4. Such experiments will
646 complement the CMIP6-PMIP4 baseline model experiments, by providing insights into whether
647 discrepancies between simulated and observed 6 ka climate could be the result of incorrect
648 specification of the land-surface boundary conditions. However, the incorporation of archaeological
649 information into LULC scenarios clearly makes it possible to target other interesting periods for such
650 experiments, for example to explore if land-use changes played a role in abrupt events such as the 4.2
651 ka event, or to examine the impact of population declines in the Americas as a consequence of
652 European colonisation (1500-1750 CE) or the changes in land use globally during the Industrial era
653 (post 1850 CE).
654

655 In addition to providing a protocol for the PMIP 6ka sensitivity experiments, we have devised a
656 protocol for implementing the optimal LULC reconstructions for the Holocene in transient climate-
657 model or ESM experiments. The goal here is to provide one of the necessary forcings that could be
658 used for transient simulations in future phases of PMIP. This will allow an assessment of LULC in
659 these simulations, and therefore help address issues that are a focus for other MIPs e.g. LUMIP or
660 LS3MIP. When these new forcings are created, they will be made available through the PMIP4
661 website (https://pmip4.lscce.ipsl.fr/doku.php/exp_design:lgm, PMIP4 repository, 2017) and the
662 ESGF Input4MIPS repository (<https://esgf-node.llnl.gov/projects/input4mips/>, with details provided
663 in the “input4MIPs summary” link). Modelling groups who run either equilibrium or transient
664 climate-model experiments following this protocol are encouraged to follow the standard CMIP
665 protocol of archiving their simulations through the ESFG.
666
667

668 **Code and Data Availability**

669 The data used for Figure 1 are publicly available. The HYDE3.2 data can be downloaded
670 <https://doi.org/10.17026/dans-25g-gez3>. The KK10 data can be downloaded from
671 <https://doi.org/10.1594/PANGAEA.871369>. The code and data used to generate Figure 1 are
672 available from https://github.com/jedokaplan/ALCC_comparison_figure. The data and code used to
673 generate Figure 3 are available from <https://github.com/mavdlind/GMD>. The data and code used to
674 generate Figure 5 are available from [10.5281/zenodo.3625226](https://doi.org/10.5281/zenodo.3625226). The European pollen-based
675 reconstructions used in Figure 7 are available <https://doi.org/10.1594/PANGAEA.897303>. The pollen
676 data used to generate the Siberian reconstructions is available from
677 <https://doi.org/10.1594/PANGAEA.898616>. An earlier version of this Figure was published in

678 Dawson et al., 2018. The code used to generate 7 Figure is available from
679 <https://doi.org/10.5281/zenodo.3604328>. The pollen-based reconstructions used in the generation of
680 Figure 8 are available from 10.5281/zenodo.3601028. The climate model outputs used to generate
681 Figure 8 are available from 10.5281/zenodo.3601040. The code used to generate Figure 8 is available
682 from 10.5281/zenodo.3601011.

683
684

685 **Acknowledgements.** LandCover 6k is a working group of the Past Global Changes (PAGES)
686 programme, which in turn received support from the Swiss Academy of Sciences. We thank PAGES
687 for their support for this activity. The land use group also received funding under the Holocene Global
688 Landuse International Focus Group of INQUA. SPH acknowledges funding from the European
689 Research Council for “GC2.0: Unlocking the past for a clearer future”. MJG thanks the Swedish
690 Strategic Research Area MERGE (Modelling the Regional and Global Earth System Model) and
691 Linnaeus University’s faculty of Health and Life Sciences (Kalmar, Sweden) for financial support.
692 We thank Joy Singarayer for providing the climate model outputs that were used to generate Figure
693 8 and Guangqi Li for assistance in producing this figure. BDS was funded by ERC H2020-MSCA-
694 IF-2015, grant number 701329. The dataset for Figure 5 was generated from the ‘Cultivating
695 Societies: Assessing the Evidence for Agriculture in Neolithic Ireland’ project, supported by the
696 Heritage Council, Ireland under the INSTAR programme 2008–2010 (Reference 16682 to
697 Whitehouse, Schulting, Bogaard and McClatchie).

698

699 **Author Contributions.** SPH, MJG, BDS, MVL, KKG wrote the first draft. SPH, PB, FSRP
700 contributed to the design of the climate model experiments, BS and TK to the design of the carbon-
701 cycle simulations. The figures were contributed by JK (Fig. 1), BS (Fig. 2, Fig 9.), MVL (Fig. 3), OB
702 (Fig. 4), NJW (Fig. 5), KKG (Fig. 6), AD (Fig. 7), SPH (Fig. 8). All authors contributed to the final
703 version of the paper.

704

705

706 **References**

- 707 Arneth, A., Denton, F., Agus, F., Elbehri, A., Erb, K., Elasha, B.O., Rahimi, M., Rounsevell, M.,
708 Spence, A., and Valentini, R.: IPCC Special Report on Climate Change, Desertification, Land
709 Degradation, Sustainable Land Management, Food Security, and Greenhouse gas fluxes in
710 Terrestrial Ecosystems, 2019.
- 711 Arneth, A., Sitch, S., Pongratz, J., Stocker, B.D., Ciais, P., Poulter, B., Bayer, A.D., Bondeau, A.,
712 Calle, L., Chini, L.P., Gasser, T., Fader, M., Friedlingstein, P., Kato, E., Li, W., Lindeskog,
713 M., Nabel, J.E.M.S., Pugh, T.A.M., Robertson, E., Viovy, N., Yue, C., and Zachle, S.:
714 Historical carbon dioxide emissions caused by land-use changes are possibly larger than
715 assumed, *Nature Geosci.*, 10, 79-84, doi: 10.1038/ngeo2882, 2017.
- 716 Balsera, V., Díaz-del-Río, P., Gilman, A., Uriarte, A., and Vicent, J.M.: Approaching the demography
717 of late prehistoric Iberia through summed calibrated probability distributions (7000-2000 cal
718 BC), *Quat. Int.*, 208-211, doi:10.106/j.quaint.2015.06.022, 2015.
- 719 Bartlein, P. J., Harrison, S. P., Brewer, S., Connor, S., Davis B. A. S., Gajewski, K., Guiot, J.,
720 Harrison-Prentice, T. I., Henderson, A., Peyron, O., Prentice, I. C., Scholze, M., Seppä, H.,
721 Shuman, B., Sugita, S., Thompson, R. S., Vial, A., Williams, J., and Wu, H.: Pollen-based
722 continental climate reconstructions at 6 and 21 ka: a global synthesis, *Clim. Dyn.*, 37, 775-
723 802, doi: 10.1007/s00382-010-0904-1, 2011.
- 724 Bartlein, P.J., Harrison, S.P., and Izumi, K.: Underlying causes of Eurasian mid-continental aridity
725 in simulations of mid-Holocene climate, *Geophys. Res. Lett.*, 44, doi:
726 10.1002/2017GL074476, 2017.

- 727 Barton, C.M., Ullah, I.I., and Bergin, S.: Land use, water and Mediterranean landscapes: modelling
728 long-term dynamics of complex socio-ecological systems, *Phil. Trans. R. Soc.*, A368, 5275-
729 5297, doi: 10.1098/rsta.2010.0193, 2010.
- 730 Berger, A., and Loutre, M-F.: Insolation values for the climate of the last 10 million of years, *Quat.*
731 *Sci. Rev.*, 10, 297-317, [https://doi.org/10.1016/0277-3791\(91\)90033-Q](https://doi.org/10.1016/0277-3791(91)90033-Q), 1991.
- 732 Bishop, R.R., Church, M.J., and Rowley-Conwy, P.A.: Firewood, food and human niche
733 construction: the potential role of Mesolithic hunter-gatherers in actively structuring
734 Scotland's woodlands, *Quat. Sci. Rev.*, 108, 51-75, 2015.
- 735 Bocquet-Appel, J.-P., Naji, S., Vander Linden, M., and Kozłowski, J.K.: Detection of diffusion and
736 contact zones of early farming in Europe from the space-time distribution of ¹⁴C dates, *J.*
737 *Arch. Sci.*, 36, 807-820, doi: 10.1016/j.jas.2008.11.004, 2009.
- 738 Crema, E.R., Habu, J., Kobayashi, K., and Madella, M.: Summed probability distribution of ¹⁴C dates
739 suggests regional divergences in the population dynamics of the Jomon period in eastern Japan,
740 *PlosOne*, 11, e0154809, doi: 10.1371/journal.pone.0154809, 2016.
- 741 Davis, B.A.S., Brewer, S., Stevenson, A.C., Guiot, J., and Juggins, S.: The temperature of Europe
742 during the Holocene reconstructed from pollen data, *Quat. Sci. Rev.*, 22, 1701–1716, 2003.
- 743 Davison, K., Dolukhanov, P., Sarson, G. R., and Shukurov, P.: The role of waterways in the spread
744 of the Neolithic, *J. Arch. Sci.*, 33, 641-652, doi: 10.106/j.jas.2005.09.017, 2006.
- 745 Dawson, A., Paciorek, C.J., McLachlan, J.S., Goring, S., Williams, J.W., and Jackson, S.T.:
746 Quantifying pollen-vegetation relationships to reconstruct ancient forests using 19th-century
747 forest composition and pollen data, *Quat. Sci. Rev.*, 137, 156-175, doi:
748 [10.1016/j.quascirev.2016.01.012](https://doi.org/10.1016/j.quascirev.2016.01.012), 2016.
- 749 Dawson, A., Cao, X., Chaput, M., Hopla, E., Li, F., Edwards, M., Fyfe, R., Gajewski, K., Goring,
750 S.J., Herzschuh, U., Mazier, F., Sugita, S., Williams, J.W., Xu, Q., and Gaillard, M-J.: Finding
751 the magnitude of human induced Northern Hemisphere land-cover transformation between 6
752 and 0.2 ka BP, *PAGES Mag.*, 26, 34-35, <https://doi.org/10.22498/pages.26.1.34>, 2018.
- 753 Egerer, S., Claussen, M., and Reick, C.: Rapid increase in simulated North Atlantic dust deposition
754 due to fast change of northwest African landscape during the Holocene, *Clim. Past*, 14, 1051-
755 1066, <https://doi.org/10.5194/cp-14-1051-2018>, 2018.
- 756 Ellis, E.C., Kaplan, J.O., Fuller, D.Q., Vavrus, S., Klein Goldewijk, K., and Verburg, P. H.: Used
757 planet: A global history, *Proc. Nat. Acad. Sci.*, 110, 7978-7985, 2013.
- 758 Elsig, J., Schmitt, J., Leuenberger, D., Schneider, R., Eyer, M., Leuenberger, M., Joos, F., Fischer,
759 H., and Stocker, T. F.: Stable isotope constraints on Holocene carbon cycle changes from an
760 Antarctic ice core, *Nature*, 461, 507-510, 2009.
- 761 Eyring, V., Bony, S., Meehl, G. A., Senior, C. A., Stevens, B., Stouffer, R. J., and Taylor, K. E.:
762 Overview of the Coupled Model Intercomparison Project Phase 6 (CMIP6) experimental design
763 and organization, *Geosci. Model Dev.*, 9, 1937–1958, [https://doi.org/10.5194/gmd-9-1937-](https://doi.org/10.5194/gmd-9-1937-2016)
764 [2016](https://doi.org/10.5194/gmd-9-1937-2016), 2016.
- 765 Fischer, N., and Jungclauss, J.H.: Evolution of the seasonal temperature cycle in a transient Holocene
766 simulation: orbital forcing and sea-ice, *Clim. Past*, 7, 1139-1148, [https://doi.org/10.5194/cp-7-](https://doi.org/10.5194/cp-7-1139-2011)
767 [1139-2011](https://doi.org/10.5194/cp-7-1139-2011), 2011.
- 768 Ford, A., and Clarke, K.C.: Linking the past and present of the ancient Maya: lowland land use,
769 population distribution, and density in the Late Classic Period, in: *The Oxford Handbook of*
770 *Historical Ecology and Applied Archaeology*, Isendahl, C. and Stump, D. (eds.), doi:
771 [10.1093/oxfordhb/9780199672691.013.33](https://doi.org/10.1093/oxfordhb/9780199672691.013.33), 2015.
- 772 Freeman, J., Baggio, J.A., Robinson, E., Byers, D.A., Gayo, E., Finley, J.B., Meyer, J.A., Kelly, R.L.,
773 and Anderies, J.M.: Synchronisation of energy consumption by human societies throughout the
774 Holocene, *Proc. Nat. Acad. Sci.*, 115, 9962-9967, doi: 10.1073/pnas.1802859115, 2018.
- 775 Fyfe R. M., Woodbridge, J. E., and Roberts, N.: From forest to farmland: pollen-inferred land cover
776 change across Europe using the pseudobiomization approach, *Glob. Change Biol.*, 21: 1197-

777 1212, doi:10.1111/gcb.12776, 2014.

778 Gaillard, M.-J., Sugita, S., Mazier, F., Kaplan, J.O., Trondman, A.-K., Brostroem, A., Hickler, T.,
779 Kjellstroem, E., Kunes, P., Lemmen, C., Olofsson, J., Smith, B., and Strandberg, G.: Holocene
780 land-cover reconstructions for studies on land-cover feedbacks, *Clim. Past*, 6, 483-499,
781 <https://doi.org/10.5194/cp-6-483-2010>, 2010.

782 Gaillard, M.-J., Whitehouse, N., Madella, M., Morrison, K., and von Gunten, L: Past land use and
783 land cover, *PAGES Mag.*, 26, 1-44, doi:10.22498/pages.26.1, 2018.

784 Harrison, S.P., Bartlein, P.J., Izumi, K., Li, G., Annan, J., Hargreaves, J., Braconnot, P.B., and
785 Kageyama, M.: Evaluation of CMIP5 palaeo-simulations to improve climate projections,
786 *Nature Clim. Change*, 5, 735-743, 2015.

787 He, F., Vavrus, S.J., Kutzbach, J.E., Ruddiman, W.F., Kaplan, J.O., and Krumhardt, K.M.: Simulating
788 global and local surface temperature changes due to Holocene anthropogenic land cover
789 change, *Geophys. Res. Lett.*, 41, 623–631, 2014.

790 Hellman, S., Gaillard, M.-J., Broström, A., and Sugita, S.: The REVEALS model, new tool to
791 estimate past regional plant abundance from pollen data in large lakes: validation in southern
792 Sweden, *J. Quat. Sci.*, 22, 1-22, 2008a.

793 Hellman, S., Gaillard M.-J., Broström, A., and Sugita, S.: Effects of the sampling design and selection
794 of parameter values on pollen-based quantitative reconstructions of regional vegetation: a case
795 study in southern Sweden using the REVEALS model, *Veg. History Archaeobot.*, 17, 445-460,
796 2008b.

797 Herrero, M., Havlik, P., Valin, H., Notenbaert, A., Rufino, M.C., Thornton, P.K., Blümmel, M.,
798 Weiss, F., Grace, D., and Obersteiner, M.: Biomass use, production, feed efficiencies, and
799 greenhouse gas emissions from global livestock systems, *Proc. Nat. Acad. Sci.*, 110, 20888-
800 20893, 2013.

801 Hughes, R.E., Weiberg, E., Bonnier, A., Finne, M., and Kaplan, J.O.: Quantifying land use in past
802 societies from cultural practice and archaeological data, *Land*, 7, 9,
803 doi.org/10.3390/land/7010009, 2018.

804 Hurtt, G., Chini, L., Sahajpal, R., Frolking, S., Calvin, K., Fujimori, S., Klein Goldewijk, K.,
805 Hasegawa, T., Havlik, P., Lawrence, D., Lawrence, P., Popp, A., Stehfest, E., van Vuuren, D.,
806 and Zhang, X.: Harmonization of global land-use change and management for the period 850–
807 2100, *Geosci. Model Dev. Discuss.*, 2017.

808 Janssen, E., Poblome, J., Claeys, J., Kint, V., Degryse, P., Marinova, E., and Muys, B.: Fuel for
809 debating ancient economies. Calculating wood consumption at urban scale in Roman Imperial
810 times, *J. Arch. Sci.: Reports*, 11, 592-599, 2017.

811 Joos, F., and Spahni, R.: Rates of change in natural and anthropogenic radiative forcing over the past
812 20,000 years, *Proc. Nat. Acad. Sci.*, 105, 1425–1430, 2008.

813 Joos, F., Gerber, S., Prentice, I.C., Otto-Bliesner, B.L., and Valdes, P.J.: Transient simulations of
814 Holocene atmospheric carbon dioxide and terrestrial carbon since the last glacial maximum,
815 *Global Biogeochem. Cy.*, 18, GB2002, doi:10.1029/2003GB002156, 2004.

816 Jungclaus, J.H., Bard, E., Baroni, M., Braconnot, P., Cao, J., Chini, L. P., Egorova, T., Evans, M.,
817 González-Rouco, J.F., Goosse, H., Hurtt, G.C., Joos, F., Kaplan, J. O., Khodri, M., Klein
818 Goldewijk, K., Krivova, N., LeGrande, A.N., Lorenz, S. J., Luterbacher, J., Man, W., Maycock,
819 A.C., Meinshausen, M., Moberg, A., Muscheler, R., Nehrbass-Ahles, C., Otto-Bliesner, B.I.,
820 Phipps, S.J., Pongratz, J., Rozanov, E., Schmidt, G.A., Schmidt, H., Schmutz, W., Schurer, A.,
821 Shapiro, A.I., Sigl, M., Smerdon, J.E., Solanki, S.K., Timmreck, C., Toohey, M., Usoskin, I.G.,
822 Wagner, S., Wu, C.-J., Yeo, K.L., Zanchettin, D., Zhang, Q., and Zorita, E.: The PMIP4
823 contribution to CMIP6 – Part 3: The last millennium, scientific objective, and experimental
824 design for the PMIP4 past1000 simulations, *Geosci. Model Dev.*, 10, 4005–4033,
825 <https://doi.org/10.5194/gmd-10-4005-2017>, 2017.

826 Kageyama, M., Braconnot, P., Harrison, S.P., Haywood, A., Jungclaus, J., Otto-Bliesner, B.,

827 Peterschmitt, J.-Y., Abe-Ouchi, A., Albani, S., Bartlein, P., Brierley, C., Crucifix, M., Dolan,
828 A., Fernandez-Donado, L., Fischer, H., Hopcroft, P., Ivanovic, R., Lambert, F., Lunt, D.,
829 Mahowald, N., Peltier, W.R., Phipps, S., Roche, D., Schmidt, G., Tarasov, L., Valdes, P.,
830 Zhang, Q., and Zhou, T.: The PMIP4 contribution to CMIP6 – Part 1: Overview and over-
831 arching analysis plan. *Geosci. Model Dev.*, 11: 1033-1057. [https://doi.org/10.5194/gmd-11-](https://doi.org/10.5194/gmd-11-1033-2018)
832 1033-2018, 2018.

833 Kaplan, J.O., Krumhardt, K.M., Ellis, E.C., Ruddiman, W.F., Lemmen, C., and Klein Goldewijk, K.:
834 Holocene carbon emissions as a result of anthropogenic land cover change, *Holocene*, 21, 775-
835 791, 2011.

836 Kaplan, J.O., Krumhardt, K.M., Gaillard, M.-J., Sugita, S., Trondman, A.-K., Fyfe, R., Marquer, L.,
837 Mazier, F., and Nielsen, A.B.: Constraining the deforestation history of Europe: Evaluation of
838 historical land use scenarios with pollen-based land cover reconstructions, *Land*, 6, 9,
839 doi:10.3390/land6040091, 2017.

840 Kaufman, D., McKay, N., Routson, C., Erb, M., Davis, B., Heiri, O., Jaccard, S., Tierney, J.,
841 Dätwyler, C., et al.: A global database of Holocene paleo-temperature records, *Scientific Data*,
842 in press.

843 Kay, A. U., Fuller, D. Q., Neumann, K., Eichhorn, B., Höhn, A., Morin-Rivat, J., Champion, L.,
844 Linseele, V., Huysecom, E., Ozainne, S., Lespez, L., Biagetti, S., Madella, M., Salzmann, U.,
845 and Kaplan, J. O.: Diversification, intensification, and specialization: Changing land use in
846 western Africa from 1800 BC to AD 1500, *J. World Prehistory*, 32, 179–228, doi:
847 [10.1007/s10963-019-09131-2](https://doi.org/10.1007/s10963-019-09131-2). 2019, 2019.

848 Klein Goldewijk, K., Beusen, A., van Drecht, G., and de Vos, M.: The HYDE 3.1 spatially explicit
849 database of human induced land use change over the past 12,000 years, *Glob. Ecol. Biogeog.*,
850 20, 73-86, 2011.

851 Klein Goldewijk, K., Beusen, A., Doelman, J., and Stehfest, E.: Anthropogenic land-use estimates
852 for the Holocene; HYDE 3.2, *Earth Syst. Sci. Data*, 9, 927-953,
853 <https://doi.org/10.5194/essd-9-927-2017>, 2017a.

854 Klein Goldewijk, K., Dekker, S.C., and van Zanden, J.L.: Per-capita estimations of long-term
855 historical land use and the consequences for global change research, *J. Land Use Sci.*, 12,
856 313-337, <https://doi.org/10.1080/1747423X.2017.1354938>, 2017b.

857 Lawrence, D.M., Hurtt, G.C., Arneth, A., Brovkin, V., Calvin, K.V., Jones, A.D., Jones, C.D.,
858 Lawrence, P.J., de Noblet-Ducoudré, N., Pongratz, J., Seneviratne, S.I., and Shevliakova, E.:
859 The Land Use Model Intercomparison Project (LUMIP) contribution to CMIP6: rationale and
860 experimental design, *Geosci. Model Dev.*, 9, 2973-2998, [https://doi.org/10.5194/gmd-9-2973-](https://doi.org/10.5194/gmd-9-2973-2016)
861 2016, 2016.

862 Le Quéré, C., Andrew, R.M., Friedlingstein, P., Sitch, S., Hauck, J., Pongratz, J., Pickers, P.A.,
863 Korsbakken, J.I., Peters, G.P., Canadell, J.G., Arneth, A., Arora, V.K., Barbero, L., Bastos, A.,
864 Bopp, L., Chevallier, F., Chini, L.P., Ciais, P., Doney, S.C., Gkritzalis, T., Goll, D.S., Harris,
865 I., Haverd, V., Hoffman, F.M., Hoppema, M., Houghton, R.A., Hurtt, G., Ilyina, T., Jain, A.K.,
866 Johannessen, T., Jones, C.D., Kato, E., Keeling, R.F., Goldewijk, K.K., Landschützer, P.,
867 Lefèvre, N., Lienert, S., Liu, Z., Lombardozzi, D., Metzl, N., Munro, D.R., Nabel, J.E.M.S.,
868 Nakaoka, S.-I., Neill, C., Olsen, A., Ono, T., Patra, P., Peregón, A., Peters, W., Peylin, P., Pfeil,
869 B., Pierrot, D., Poulter, B., Rehder, G., Resplandy, L., Robertson, E., Rocher, M., Rödenbeck,
870 C., Schuster, U., Schwinger, J., Séférian, R., Skjelvan, I., Steinhoff, T., Sutton, A., Tans, P.P.,
871 Tian, H., Tilbrook, B., Tubiello, F. N., van der Laan-Luijkx, I.T., van der Werf, G.R., Viovy,
872 N., Walker, A.P., Wiltshire, A.J., Wright, R., Zaehle, S., and Zheng, B.: Global Carbon Budget
873 2018, *Earth Syst. Sci. Data*, 10, 2141-2194, <https://doi.org/10.5194/essd-10-2141-2018>, 2018.

874 Loisel, J., Yu, Z., Beilman, D.W., Camill, P., Alm, J., Amesbury, M.J., Anderson, D., Andersson, S.,
875 Bochicchio, C., Barber, K., Belyea, L.R., Bunbury, J., Chambers, F.M., Charman, D.J.,
876 Vleeschouwer, F.D., Fiałkiewicz-Kozieł, B., Finkelstein, S.A., Gałka, M., Garneau, M.,

877 Hammarlund, D., Hinchcliffe, W., Holmquist, J., Hughes, P., Jones, M.C., Klein, E.S., Kokfelt,
878 U., Korhola, A., Kuhry, P., Lamarre, A., Lamentowicz, M., Large, D., Lavoie, M., MacDonald,
879 G., Magnan, G., Mäkilä, M., Mallon, G., Mathijssen, P., Mauquoy, D., McCarroll, J., Moore,
880 T.R., Nichols, J., O'Reilly, B., Oksanen, P., Packalen, M., Peteet, D., Richard, P.J., Robinson,
881 S., Ronkainen, T., Rundgren, M., Sannel, A.B.K., Tarnocai, C., Thom, T., Tuittila, E.-S.,
882 Turetsky, M., Väiliranta, M., and der Linden, M., van Geel B., van Bellen, S., Vitt, D., Zhao,
883 Y., and Zhou, W.: A database and synthesis of northern peatland soil properties and Holocene
884 carbon and nitrogen accumulation, *Holocene*, 24, 1028-1042, 2014.

885 Lyman, R. L.: *Quantitative Paleozoology*. Cambridge University Press, 2008.

886 Maezumi, S.Y., Robinson, M., de Souza, J., Urrego, D.H., Schaan, D., Alves, D., and Iriarte, J.: New
887 insights from pre-Columbian land use and fire management in Amazonian Dark Earth forests,
888 *Front. Ecol. Evol.*, 6, 111, doi: 10.3389/fevo.2018.00111, 2018.

889 Mahowald, N.M., Randerson, J.T., Lindsay, K., Munoz, E., Doney, S.C., Lawrence, P.,
890 Schlunegger, S., Ward, D.S., Lawrence, D., and Hoffman, F. M.: Interactions between land use
891 change and carbon cycle feedbacks, *Glob. Biogeochem. Cy.*, 31, 96–113,
892 doi:10.1002/2016GB005374, 2017.

893 Marston, J.M.: Modeling wood acquisition strategies from archaeological charcoal remains, *J. Arch.*
894 *Sci.*, 36, 2192-2200, 2009.

895 Marston, J.M., Holdaway, S.J., and Wendrich, W.: Early- and middle-Holocene wood exploitation in
896 the Fayum basin, Egypt, *Holocene*, 27, 1812-1824, 2017.

897 Mauri, A., Davis, B. A. S., Collins, P. M., and Kaplan, J. O.: The influence of atmospheric circulation
898 on the mid-Holocene climate of Europe: a data–model comparison, *Clim. Past*, 10, 1925–1938,
899 <https://doi.org/10.5194/cp-10-1925-2014>, 2014.

900 Mazoyer, M., and Roudart, L.: *A History of World Agriculture: From the Neolithic to the Current*
901 *Crisis*. Earthscan, UK, 2006.

902 McGrath, M. J., Luyssaert, S., Meyfroidt, P., Kaplan, J. O., Burgi, M., Chen, Y., Erb, K., Gimmi, U.,
903 McInerney, D., Naudts, K., Otto, J., Pasztor, F., Ryder, J., Schelhaas, M. J., and Valade, A.:
904 Reconstructing European forest management from 1600 to 2010, *Biogeosci.*, 12, 4291-4316.
905 doi:10.5194/bg-12-4291-2015, 2015.

906 McLaughlin, T. R., Whitehouse, N. J., Schulting, R. J., McClatchie, M., Barratt, P. and Bogaard, A.:
907 The changing face of Neolithic and Bronze Age Ireland: A big data approach to the
908 settlement and burial records. *J. World Prehist.*, 29, 117-153. doi:10.1007/s10963-016-
909 9093-0, 2016.

910 Messori, G., Gaetani, M., Zhang, Q., Zhang, Q., and Pausata, F. S. R.: The water cycle of the mid-
911 Holocene West African monsoon: The role of vegetation and dust emission changes, *Int. J.*
912 *Climatol.*, 39, 1927– 1939, <https://doi.org/10.1002/joc.5924>, 2019.

913 Mitchell, L., Brook, E., Lee, J., Buizert, C., and Sowers, T.: Constraints on the late Holocene
914 anthropogenic contribution to the atmospheric methane budget, *Science*, 342, 964–966,
915 doi:10.1126/science.1238920, 2013.

916 Morrison, K.D., Hammer, E., Popova, L., Madella, M., Whitehouse, N., Gaillard, M.-J. and
917 LandCover6k Land-Use Group Members: Global-scale comparisons of human land use:
918 developing shared terminology for land-use practices for global changes, *PAGES Mag.*, 26, 8-
919 9, 2018.

920 Myhre, G., Shindell, D., Bréon, F.-M., Collins, W., Fuglestedt, J., Huang, J., Koch, D., Lamarque,
921 J.-F., Lee, D., Mendoza, B., Nakajima, T., Robock, A., Stephens, G., Takemura T., and Zhang,
922 H.: Anthropogenic and natural radiative forcing. in: *Climate Change 2013: The Physical*
923 *Science Basis*. Contribution of Working Group I to the Fifth Assessment Report of the
924 Intergovernmental Panel on Climate Change (T F Stocker, D Qin, G-K Plattner, M Tignor, S
925 K Allen, J Boschung, A Nauels, Y Xia, V Bex and P M Midgley (eds), Cambridge: Cambridge
926 University Press Cambridge, United Kingdom and New York, NY, USA, 2013.

- 927 Nakagawa, T., Tarasov, P.E., Nishida, K., Gotanda, K., and Yasuda, Y.: Quantitative pollen-based
 928 climate reconstruction in central Japan: application to surface and Late Quaternary spectra,
 929 *Quat. Sci. Rev.*, 21, 2099–2113, 2002.
- 930 Nielsen, A.B., Giesecke, T., Theuerkauf, M., Feeser, I., Behre, K.-H., Beug, H.-J., Chen, S.-H.,
 931 Christiansen, J., Dörfler, W., Endtmann, E., Jahns, S., de Klerk, O., Köhl, N., Latałowa, M.,
 932 Odgaard, B.V., Rasmussen, P., Stockholm, J.R., Voigt, R., Wiethold, J., and Wolters, S.:
 933 Quantitative reconstructions of changes in regional openness in north-central Europe reveal
 934 new insights into old questions, *Quat. Sci. Rev.*, 47, 131–149, 2012.
- 935 Oh, Y., Conte, M., Kang, S., Kim, J., and Hwang, J.: Population fluctuation and the adoption of food
 936 production in prehistoric Korea: using radiocarbon dates as a proxy for population change,
 937 *Radiocarbon*, 59, 1761-1770, doi: 10.1017/RDC.2017.1.22, 2017.
- 938 Ortega-Rosas, C.I., Guiot, J., Penalba, M.C., Ortiz-Acosta, M.E.: Biomization and quantitative
 939 climate reconstruction techniques in northwestern Mexico—with an application to four
 940 Holocene pollen sequences, *Glob. Planet. Change*, 61, 242–266, 2008.
- 941 Orton, D., Gaastra, J., and Vander Linden, M.: Between the Danube and the Deep Blue Sea:
 942 zooarchaeological meta-analysis reveals variability in the spread and development of Neolithic
 943 farming across the western Balkans, *Open Quat.*, 2, doi: 10.5334/oq.28, 2016.
- 944 Otto-Bliesner, B.L., Braconnot, P., Harrison, S.P., Lunt, D.J., Abe-Ouchi, A., Albani, S., Bartlein,
 945 P.J., Capron, E., Carlson, A.E., Dutton, A., Fischer, H., Goelzer, H., Govin, A., Haywood, A.,
 946 Joos, F., Legrande, A.N., Lipscomb, W.H., Lohmann, G., Mahowald, N., Nehrbass-Ahles, C.,
 947 Pausata, F.S.R., Peterschmidt, J.-Y., Phipps, S.J., Renssen, R., and Zhang, Q.: The PMIP4
 948 contribution to CMIP6 – Part 2: Two interglacials, scientific objective and experimental design
 949 for Holocene and Last Interglacial simulations. *Geosci. Mod. Dev.*, 10, 3979-4003,
 950 <https://doi.org/10.5194/gmd-10-1-2017>, 2017.
- 951 Pausata, F.S.R., Messori, G., Zhang, Q.: Impacts of dust reduction on the northward expansion of the
 952 African monsoon during the Green Sahara period, *Earth Planet. Sci. Lett.*, 434, 298-
 953 307, <https://doi.org/10.1016/j.epsl.2015.11.049>, 2016.
- 954 Perugini, L., Caporaso, L., Marconi, S., Cescatti, A., Quesada, B., de Noblet-Ducoudré, N., House,
 955 J.I., and Arneeth, A.: Biophysical effects on temperature and precipitation due to land cover
 956 change, *Environ. Research Lett.*, 12, 053002, <https://doi.org/10.1088/1748-9326/aa6b3f>, 2017.
- 957 Phelps, L.N., and Kaplan, J.O.: Land use for animal production in global change studies: Defining
 958 and characterizing a framework, *Glob Chang Biol*, 23, 4457-4471, 10.1111/gcb.13732, 2017.
- 959 Pirzamanbein, B., Lindström, J., Poska, A., Sugita, S., Trondman, A., Fyfe, R., Mazier, F., Nielsen,
 960 A.B., Kaplan, J.O., Bjune, A.E., Birks, H.J.B., Giesecke, T., Kangur, M., Latałowa, M.,
 961 Marquer, L., Smith, B., and Gaillard, M.-J.: Creating spatially continuous maps of past land
 962 cover from point estimates: A new statistical approach applied to pollen data, *Ecol. Complexity*,
 963 20, 127-141, 2014.
- 964 Pirzamanbein, B., Lindström, J., Poska, A., and Gaillard, M.-J.: Modelling spatial compositional data:
 965 Reconstructions of past land cover and uncertainties, *Spatial Stat.*, 24, 14–31, 2018.
- 966 Pongratz, J., Reick, C., Raddatz, T., and Claussen, M.: A reconstruction of global agricultural areas
 967 and land cover for the last millennium, *Glob. Biogeochem. Cy.*, 22, 2008.
- 968 Pongratz, J., Reick, C.H., Raddatz, T., and Claussen, M.: Biogeophysical versus biogeochemical
 969 climate response to historical anthropogenic land cover change, *Geophys. Res. Lett.*, 37,
 970 L08702, doi:10.1029/2010GL043010, 2010.
- 971 Pongratz, J., Reick, C. H., Houghton, R. A., and J. I. House, J. I.: Terminology as a key uncertainty
 972 in net land use and land cover change carbon flux estimates, *Earth Syst. Dynam.*, 5, 177–195,
 973 www.earth-syst-dynam.net/5/177/2014/ doi:10.5194/esd-5-177-2014, 2014.
- 974 Ramankutty, N., and Foley, J.A.: Estimating historical changes in global land cover: Croplands from
 975 1700 to 1992, *Glob. Biogeochem. Cy.*, 13, 997-1027, 1999.
- 976 Reitz, E. J., and Wing E.S.: Zooarchaeology. Cambridge University Press, 2008.

- 977 Rick, J.W.: Dates as data: an examination of the Peruvian Pre-ceramic radiocarbon record, *Am. Antiq.*,
978 52, 55–73, 1987.
- 979 Robinson, E., Zahid, H.J., Coddling, B.F., Haas, R., and Kelly, R.L.: Spatiotemporal dynamics of
980 prehistoric human population growth: radiocarbon ‘dates as data’ and population ecology
981 models, *J. Arch. Sci.*, 101, 63–71, 2019.
- 982 Ruddiman, W. F.: The anthropogenic greenhouse era began thousands of years ago, *Clim. Change*,
983 61, 261–293, doi:10.1023/B:CLIM.0000004577.17928.fa, 2003.
- 984 Russell, T., Silva, F., and Steele, J.: Modelling the spread of farming in the Bantu-speaking regions
985 of Africa: an archaeology-based phylogeography, *PlosONE*, 9, e87584, doi:
986 10.1371/journal.pone.0087584, 2014.
- 987 Shennan, S., Downey, S.S., Timpson, A., Edinborough, K., Colledge, S., Kerig, T., Manning, K., and
988 Thomas, M.G.: Regional population collapse followed initial agriculture booms in mid-
989 Holocene Europe, *Nat. Comms.*, 4, 248, doi: 10.1038/ncomms3486, 2013.
- 990 Shevliakova, E., Pacala, S. W., Malyshev, S., Hurtt, G. C., Milly, P. C. D., Caspersen, J. P., Sentman,
991 L. T., Fisk, J. P., Wirth, C., and Crevoisier, C.: Carbon cycling under 300 years of land use
992 change: Importance of the secondary vegetation sink, *Glob. Biogeochem. Cy.*, 23, GB2022,
993 doi:10.1029/2007GB003176, 2009.
- 994 Sigl, M., Winstrup, M., McConnell, J.R., Welten, K.C., Plunkett, G., Ludlow, F., Büntgen, U., Caffee,
995 M., Chellman, N., Dahl-Jensen, D., Fischer, H., Kipfstuhl, S., Kostick, C., Maselli, O.J.,
996 Mekhaldi, F., Mulvaney, R., Muscheler, R., Pasteris, D.R., Pilcher, J.R., Salzer, M., Schüpbach,
997 S., Steffensen, J.P., Vinther, B.M., and Woodruff, T.E.: Timing and climate forcing of volcanic
998 eruptions for the past 2,500 years, *Nature*, 523, 543–549, <https://doi.org/10.1038/nature14565>,
999 2015.
- 1000 Silva, F., and Steele, J.: New methods for reconstructing geographical effects on dispersal rates from
1001 large-scale radiocarbon databases, *J. Arch. Sci.*, 52, 609–620, doi: 10.1016/j.jas.2014.04.021,
1002 2014.
- 1003 Silva, F., and Vander Linden, M.: Amplitude of travelling front as inferred from ¹⁴C predicts levels
1004 of genetic admixture among European early farmers, *Sci. Reports*, 7, 11985, doi:
1005 10.1038/s41598-017-12318-2, 2017.
- 1006 Silva, F., Stevens, C.J., Weisskopf, A., Castillo, C., Qin, L., Bevan, A., and Fuller, D.Q.: Modelling
1007 the geographical origin of rice cultivation in Asia using the Rice Archaeological Database,
1008 *PlosOne*, 10, e0137024, 2015.
- 1009 Singarayer, J.S., Valdes, P.J., Friedlingstein, P., Nelson, S., and Beerling, D.J.: Late Holocene
1010 methane rise caused by orbitally controlled increase in tropical sources, *Nature*, 470, 82– 85,
1011 doi:10.1038/nature09739, 2011.
- 1012 Smith, M.C., Singarayer, J.S., Valdes, P.J., Kaplan, J.O., and Branch, N.P.: The biogeophysical
1013 climatic impacts of anthropogenic land use change during the Holocene, *Clim. Past*, 12, 923–
1014 941, doi: <https://doi.org/10.5194/cp-12-923-2016>, 2016.
- 1015 Steinhilber, F., Abreu, J. A., Beer, J., Brunner, I., Christl, M., Fischer, H., Heikkilä, U., Kubik, P. W.,
1016 Mann, M., McCracken, K.G., Miller, H., Miyahara, H., Oerter, H., and Wilhelms, F.: 9400
1017 years of cosmic radiation and solar activity from ice cores and tree rings, *Proc. Natl. Acad. Sci.*,
1018 109, 5967–5971, 2012.
- 1019 Stocker, B. D., Strassmann, K., and Joos, F.: Sensitivity of Holocene atmospheric CO₂ and the
1020 modern carbon budget to early human land use: analyses with a process-based model,
1021 *Biogeosci.*, 8, 69–88, doi:10.5194/bg-8-69-2011, 2011.
- 1022 Stocker, B.D., Yu, Z., Massa, C., and Joos, F.: Holocene peatland and ice-core data constraints on
1023 the timing and magnitude of CO₂ emissions from past land use, *Proc. Natl. Acad. Sci.*, 114,
1024 1492–1497, doi:10.1073/pnas.1613889114, 2017.
- 1025 Styring, A., Rösch, M., Stephan, E., Stika, H.-P., Fischer, E., Sillmann, E., and Bogaard, A.:
1026 Centralisation and long-term change in farming regimes: comparing agricultural practices in

- 1027 Neolithic and Iron Age south-west Germany, *Proc. Prehist. Soc.*, 83: 357-381, doi:
 1028 10.1017/ppr.2017.3, 2017.
- 1029 Sugita, S.: Theory of quantitative reconstruction of vegetation I: pollen from large sites REVEALS
 1030 regional vegetation composition, *Holocene*, 17, 229–241, 2007.
- 1031 Tarasov, P., Williams, J.W., Andreev, A., Nakagawa, T., Bezrukova, E., Herzs Schuh, U., Igarashi, Y.,
 1032 Müller, S., Werner, K., and Zheng, Z.: Satellite- and pollen-based quantitative woody cover
 1033 reconstructions for northern Asia: Verification and application to late-Quaternary pollen data,
 1034 *Earth Planet. Sci. Lett.*, 264, 284–298, 2007.
- 1035 Tauger, M.B: *Agriculture in World History*, Routledge, 2013.
- 1036 Tierney, J.E., Pausata, F.S.R., and deMenocal, P.B.: Rainfall regimes of the Green Sahara, *Sci.*
 1037 *Advan.*, 3, e1601503, 2017.
- 1038 Timpson, A., Colledge, S., Crema, E., Edinborough, K., Kerig, T., Manning, K., Thomas, M. G. &
 1039 Shennan, S.: Reconstructing regional population fluctuations in the European Neolithic using
 1040 radiocarbon dates: a new case-study using an improved method, *J. Arch. Sci.*, 52, 549-557, doi:
 1041 10.1016/j.jas.2014.08.011, 2014.
- 1042 Toohey, M. and Sigl, M.: Volcanic stratospheric sulphur injections and aerosol optical depth from
 1043 500 BCE to 1900 CE, *Earth Syst. Sci. Data*, 9, 809-831, [https://doi.org/10.5194/essd-9-809-](https://doi.org/10.5194/essd-9-809-2017)
 1044 [2017](https://doi.org/10.5194/essd-9-809-2017), 2017.
- 1045 Trondman, A. K., Gaillard, M.-J., Mazier, F., Sugita, S., Fyfe, R., Nielsen, A.B., Twiddle, C., Barratt,
 1046 P., Birks, H.J.B., Bjune, A. E., Björkman, L., Broström, A., Caseldine, C., David, R., Dodson,
 1047 J., Dörfler, W., Fischer, E., van Geel, B., Giesecke, T., Hultberg, T., Kalnina, L., Kangur, M.,
 1048 van der Knaap, P., Koff, T., Kuneš, P., Lagerås, P., Latałowa, M., Lechterbeck, J., Leroyer, C.,
 1049 Leydet, M., Lindbladh, M., Marquer, L., Mitchell, F.J. G., Odgaard, B.V., Peglar, S.M.,
 1050 Persson, T., Poska, A., Rösch, M., Seppä, H., Veski, S., and Wick, L.: Pollen-based quantitative
 1051 reconstructions of Holocene regional vegetation cover (plant-functional types and land-cover
 1052 types) in Europe suitable for climate modelling, *Glob. Change Biol.*, 21, 676-697,
 1053 doi:10.1111/gcb.12737, 2015.
- 1054 Trondman, A.-K., Gaillard, M.-J., Sugita, S., Björkman, L., Greisman, A., Hultberg, T., Lagerås, P.,
 1055 and Lindbladh, M.: Are pollen records from small sites appropriate for REVEALS model-based
 1056 quantitative reconstructions of past regional vegetation? An empirical test in southern Sweden,
 1057 *Veget. Hist. Archaeobot.*, 25, 131–151, doi: 10.1007/s00334-015-0536-9, 2016.
- 1058 van den Hurk, B., Kim, H., Krinner, G., Seneviratne, S.I., Derksen, C., Oki, T., Douville, H., Colin,
 1059 J., Ducharne, A., Cheruy, F., Viovy, N., Puma, M.J., Wada, Y., Li, W., Jia, B., Alessandri, A.,
 1060 Lawrence, D.M., Weedon, G.P., Ellis, R., Hagemann, S., Mao, J., Flanner, M.G., Zampieri, M.,
 1061 Materia, S., Law, R.M., and Sheffield, J.: LS3MIP (v1.0) contribution to CMIP6: the Land
 1062 Surface, Snow and Soil moisture Model Intercomparison Project – aims, setup and expected
 1063 outcome, *Geosci. Model Dev.*, 9, 2809-2832, <https://doi.org/10.5194/gmd-9-2809-2016>, 2016.
- 1064 Vavrus, S., Ruddiman, W.F., and Kutzbach, J.E.: Climate model tests of the anthropogenic influence
 1065 on greenhouse-induced climate change: the role of early human agriculture, industrialization,
 1066 and vegetation feedbacks, *Quat. Sci. Rev.*, 27, 1410-1425, 2008.
- 1067 Veal, R., 2017. Wood and charcoal for Rome: towards an understanding of ancient regional fuel
 1068 economics, In de Haas, T. & Gijs, T. (eds), *Rural communities in a globalizing economy: new*
 1069 *perspectives on the economic integration of Roman Italy*, Brill, (New York and Leiden):
 1070 pp.388-406.
- 1071 Viau, A.E., and Gajewski, K.: Reconstructing millennial, regional paleoclimates of boreal Canada
 1072 during the Holocene, *J. Clim.*, 22, 316–330, 2009.
- 1073 Viau, A., Gajewski, K., Sawada, M., and Fines, P.: Mean-continental July temperature variability in
 1074 North America during the past 14,000 years, *J. Geophys. Res. Atmos.*, 111, D09102,
 1075 doi:10.1029/2005JD006031, 2006
- 1076 Weiberg, E., Hughes, R. E., Finné, M., Bonnier, A., and Kaplan, J. O.: Mediterranean land use

1077 systems from prehistory to antiquity: a case study from Peloponnese (Greece), *J. Land Use Sci.*,
1078 1-20, doi:10.1080/1747423x.2019.1639836, 2019.

1079 Whitehouse, N., Schulting, R. J., McClatchie, M., Barratt, P., LcLaughlin, T.R., Bogaard, A.,
1080 Colledge, S., Marchant, R., Gaffrey, J., and Bunting, M.J.: Neolithic agriculture on the
1081 European western frontier: the boom and bust of early farming in Ireland, *J. Arch. Sci.*, 51, 181-
1082 205, doi: 10.1016/j.jas.2013.08.009, 2014.

1083 Williams, A.: The use of summed radiocarbon probability distributions in archaeology: a review of
1084 methods. *J. Archaeol. Sci.*, 39, 578–589, <https://doi.org/10.1016/j.jas.2011.07.014>, 2012.

1085 Wilmshurst, J.M., McGlone, M.S., Leathwick, J.R., and Newnham, R.M.: A pre-deforestation pollen-
1086 climate calibration model for New Zealand and quantitative temperature reconstructions for the
1087 past 18000 years BP, *J. Quat. Sci.*, 22, 535–547, 2007.

1088 Wright, P.: Preservation or destruction of plant remains by carbonization. *J.Arch.Sci* 30, 577-583,
1089 doi: 10.1016/S0305-4403(02)00203-0, 2003.

1090 Zahid, H.J., Robinson, E., and Kelly, R.L.: Agriculture, population growth, and statistical analysis of
1091 the radiocarbon record, *Proc. Natl. Acad. Sci.*, 113, 931-935, doi: 10.1073/pnas.1517650112,
1092 2016.

1093 Zanon, M., Davis, B.A.S., Marquer, L., Brewer, S., and Kaplan, J.O.: European forest cover during
1094 the past 12,000 years: a palynological reconstruction based on modern analogs and remote
1095 sensing, *Front. Plant Sci.*, 9, 253, doi: 10.3389/fpls.201800253, 2018.

1096 Zimmermann, A., Wendt, K.P., and Hilpert, J.: Landscape archaeology in central Europe. *Proc.*
1097 *Prehist. Soc.*, 75, 1-53, doi: 10.1017/S007949X00000281, 2009.

1098 Zohary, D., Hopf, M., and Weiss, E.: *Domestication of Plants in the Old World: The Origin and*
1099 *Spread of Domesticated Plants in South-west Asia, Europe, and the Mediterranean Basin*, 4th
1100 Edn., Oxford University Press, Oxford, 2012.